Scanning probe microscopy

PH 673

Nanoscience and nanotechnology

November 17, 2025

A Bit of Microscopy History

Optical Microscope
~1700

SEM: 1942

Electrons: TEM
1931

1981: STM

1986: AFM

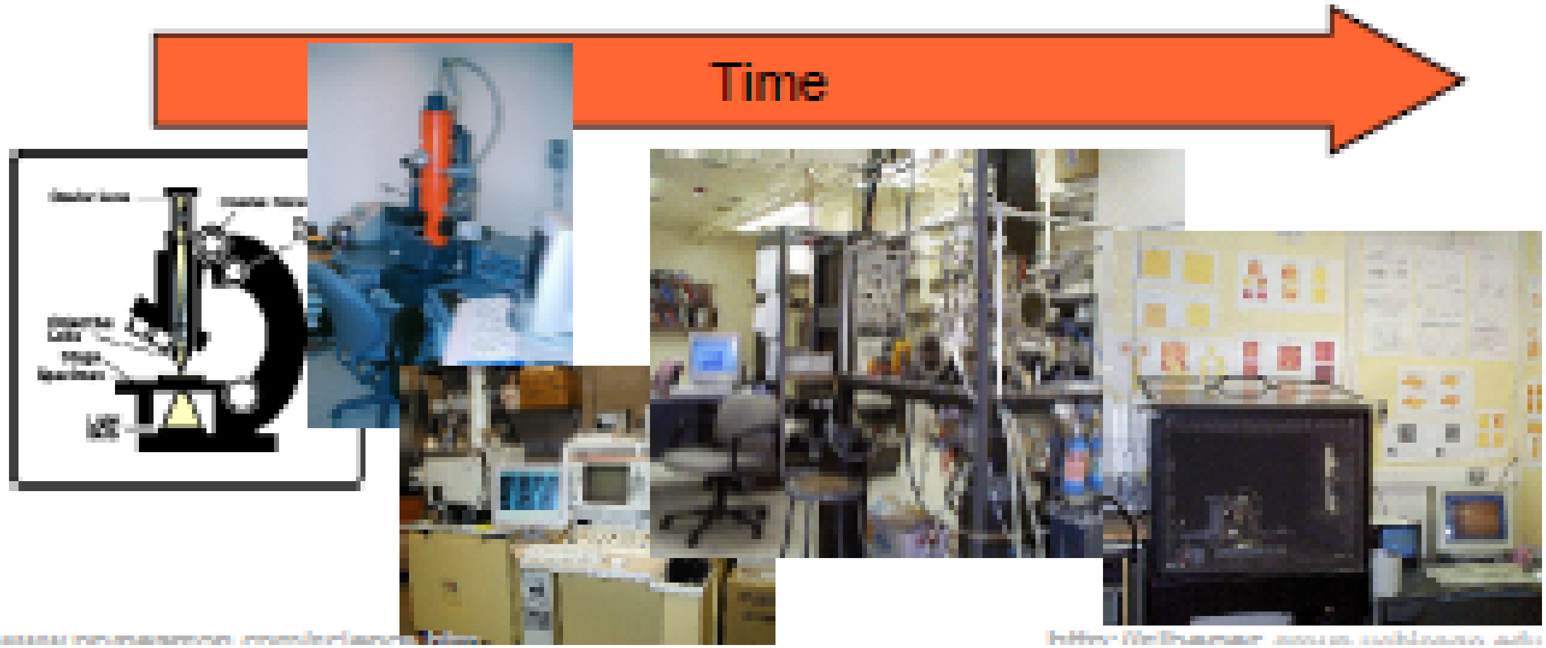

Biological and Electronic Component Dimensions

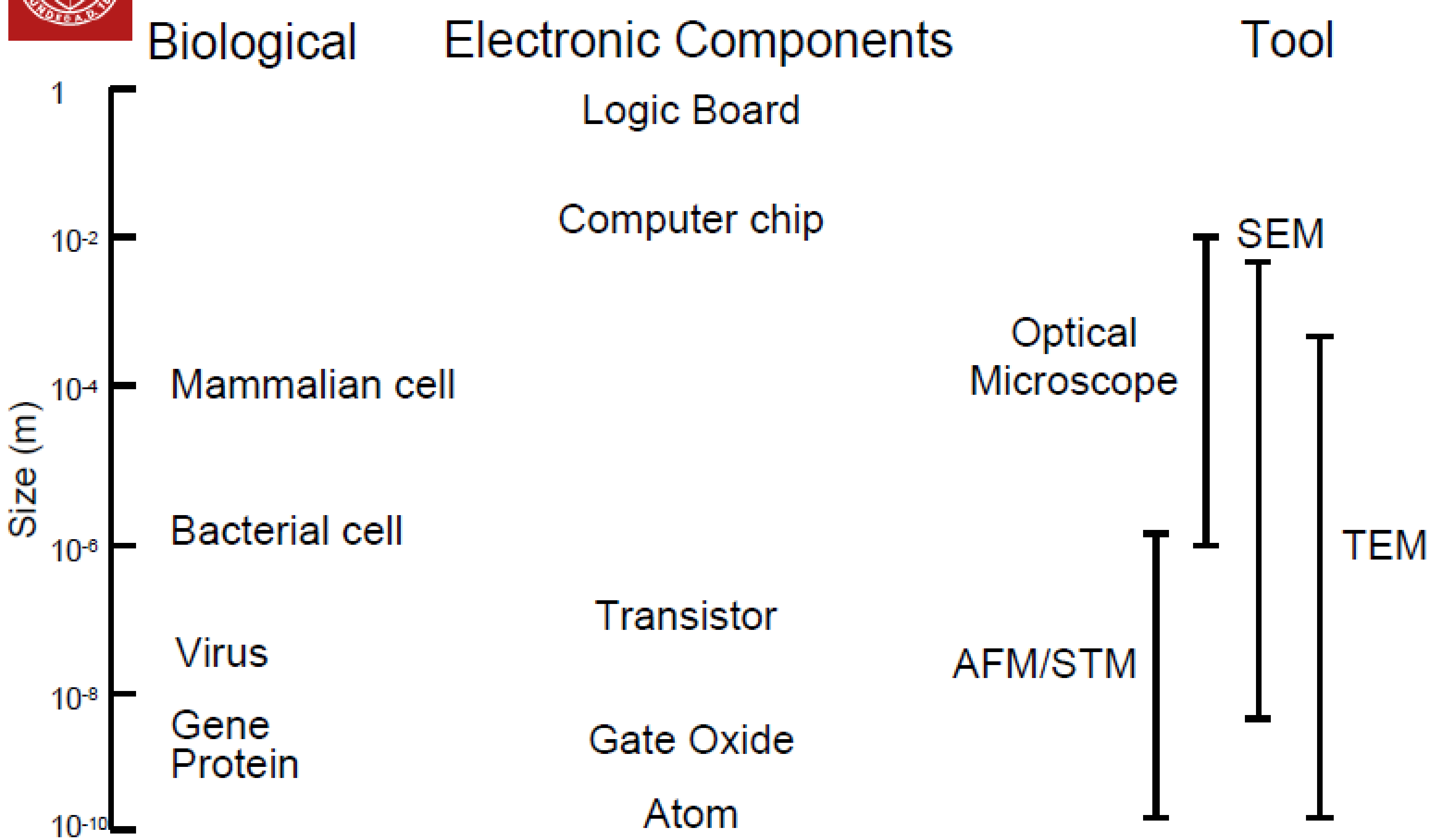

Scanning probe microscopies

STM was born in 1981:
Gerd Binning and Heinrich Rohrer,
Nobel prize 1986
AFM was born in 1986:
Gerd Binning and co-workers

Scanning probe microscopy has been essential in the development of nanotechnology:
Characterisation/visualisation tool at nanoscale.
Nanomanipulator and modificator.

Nanometer = 10^{-9} m
dimension of a few atoms cluster

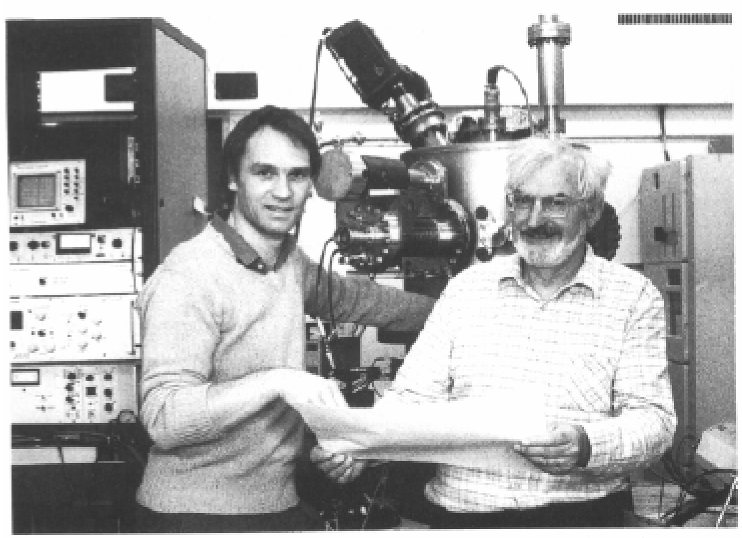

Gerd Binnig (left) and Heinrich Rohrer (right) who were awarded the Nobel Prize for their invention of the scanning tunneling microscope.

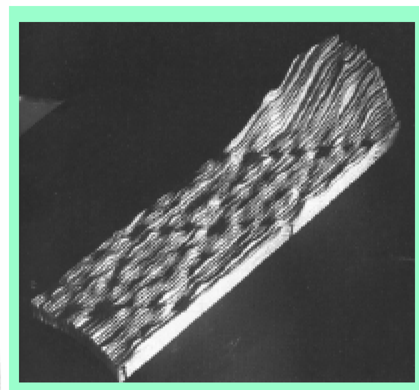

Si 7x7 surface reconstruction

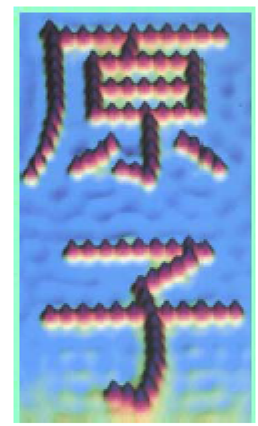

Japanese word "atom"

SPM Timeline

- 1981 First STM results in the lab
- 1982 First PRL, Atomic steps on Au(110), Si(111)7x7 in '83
- 1984 Near field optical microscope
- 1985 First atomic resolution results by others
- 1985 Invention of AFM at Stanford
- 1986 Nobel Prize for Ruska, Binnig & Rohrer
  - first STM built at LBL (Miquel Salmeron, Joe Katz, Dan Coulomb Greg Blackman)
- 1987 First commercial instruments
  - Spin-offs from Quate group in Stanford (Park), Hansma group in UCSB (DI)
  - first computerized STM at LBL, maybe anywhere… (RHK/McAllister)
- 1989 First AFM and first UHV STM at LBL
  - Bill Kolbe
- 1991 first year > 1000 STM papers published
  - commercial instruments that work…
- ~ 1995 AFM widely used in industry, SPM widely used by non-specialist groups
- Over 2,000 STM and 6,500 AFM papers per year in the 1995-2000

There are two types of **Scanning Probe Microscopies:**

Principle: bringing a very sharp probe close to the surface.

Scanning Tunnelling Microscopy (STM):

Probe does not touch the surface.
Maintains a constant tunnelling electrical current.
Very high resolution (x-y: 0.1 nm, z: 0.01 nm).
Limited to conducting materials.

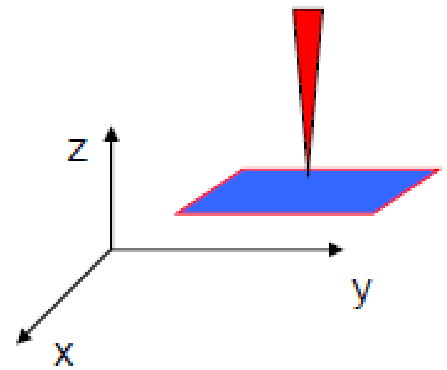

Atomic Force Microscopy (AFM):

Probe can touch the surface.
Maintains a constant very small force.
High resolution (x-y: 2-10 nm, z: 0.1 nm)
Suitable for all surfaces.

STM: better resolution but limited to conducting materials
AFM: worse resolution but all types of surfaces

STM: scanning tunneling microscope

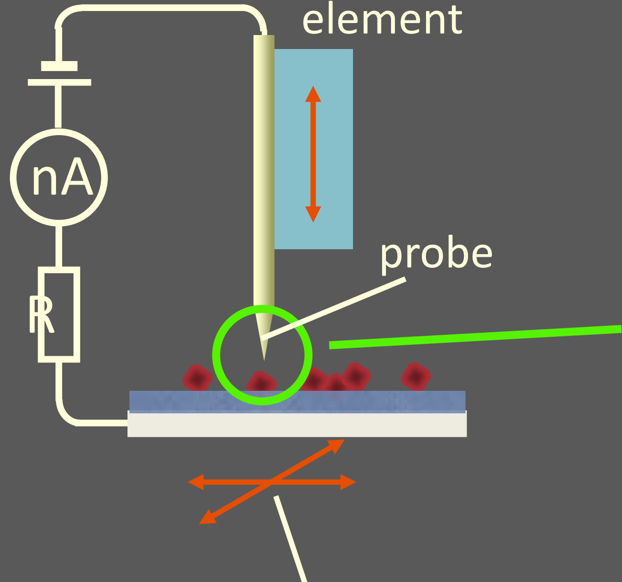

tunneling of electrons through air between probe and surface

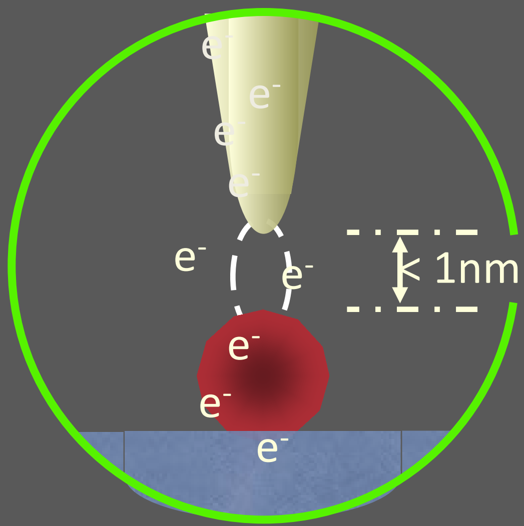

only conducting material

AFM: atomic force microscope

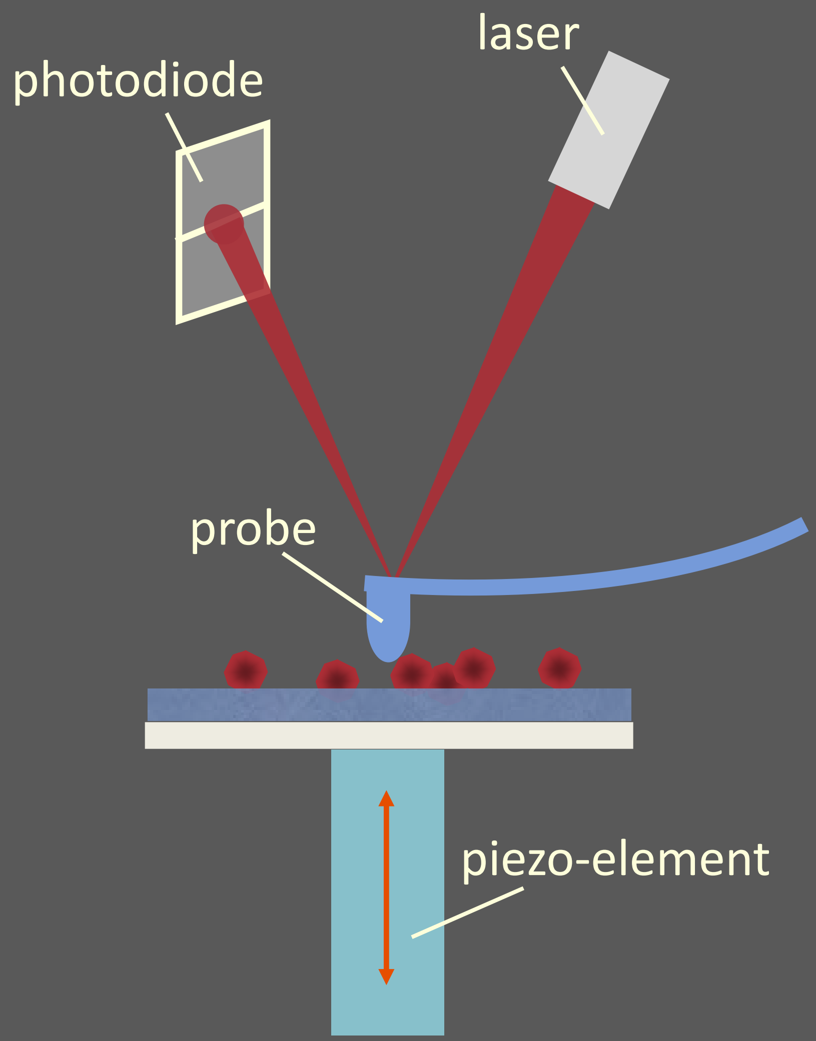

Liquids, thin films, etc.

MFM: magnetic force microscope

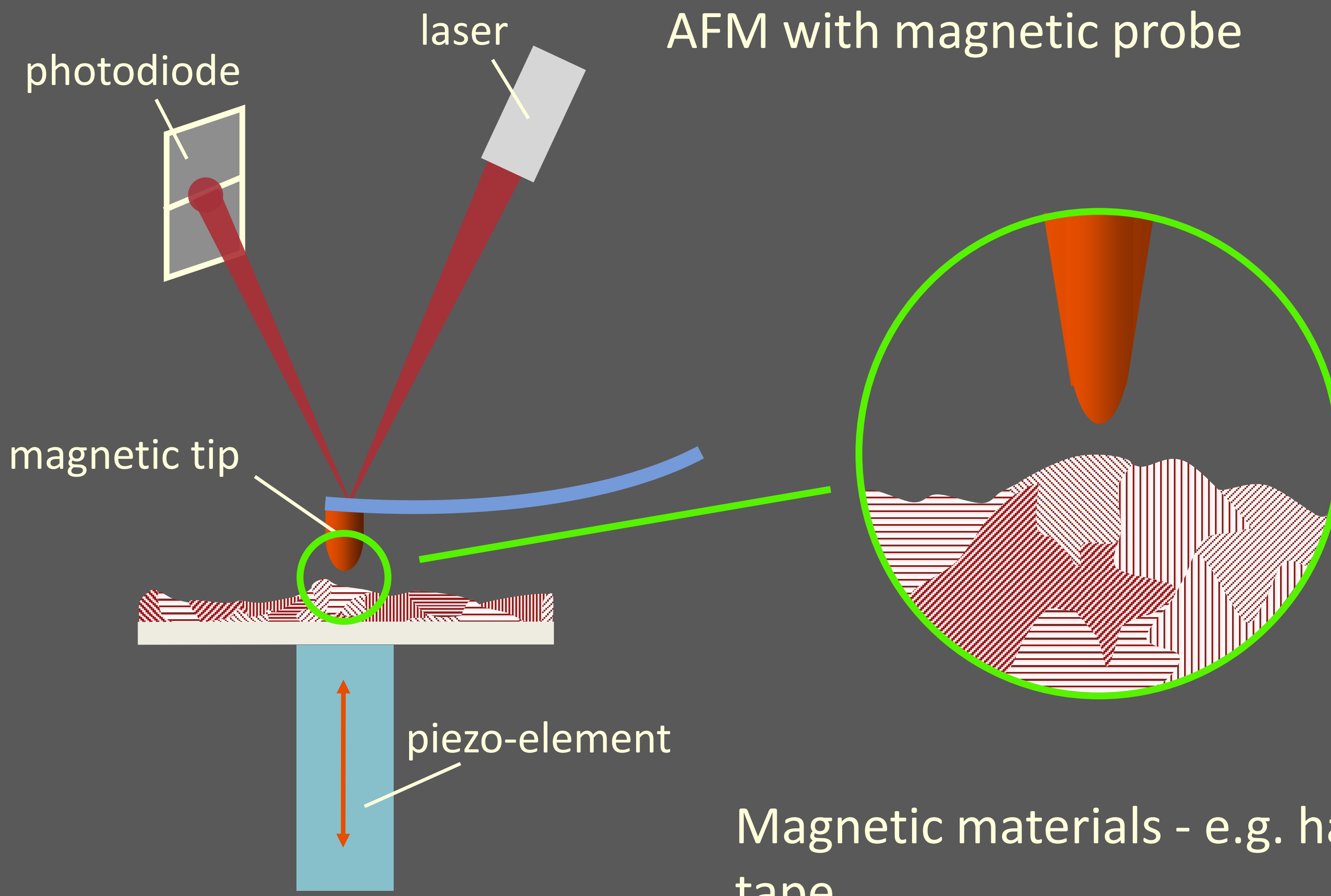

Magnetic materials - e.g. hard disc, tape

SNOM: scanning near-field optical microscope

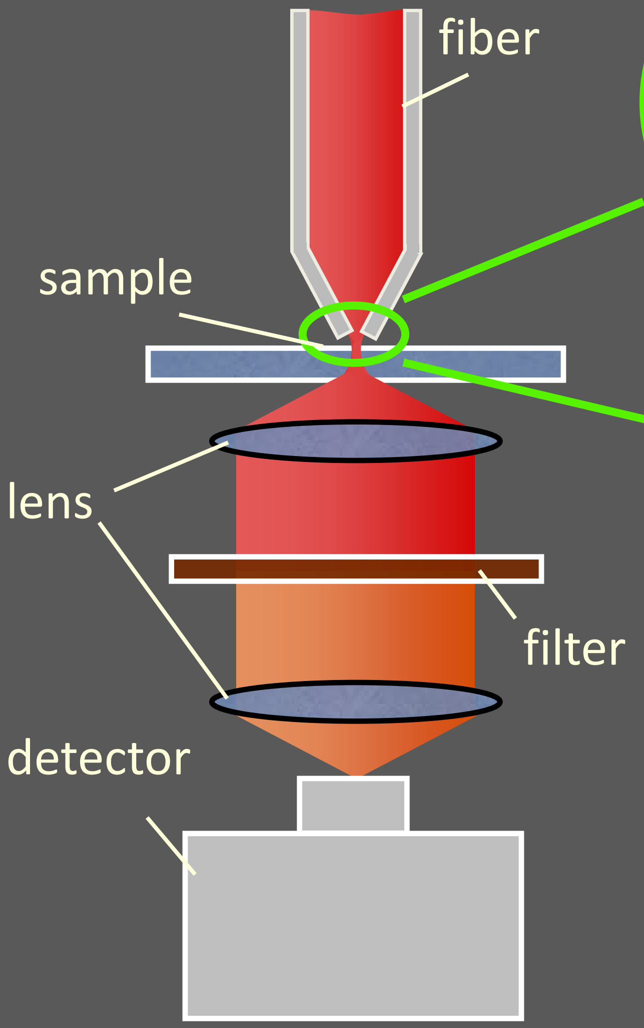

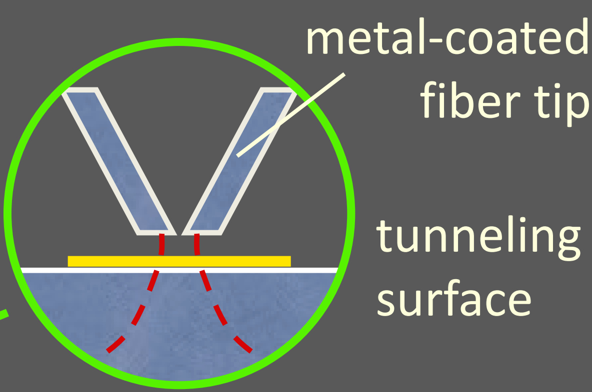

tunneling of photons between probe and surface

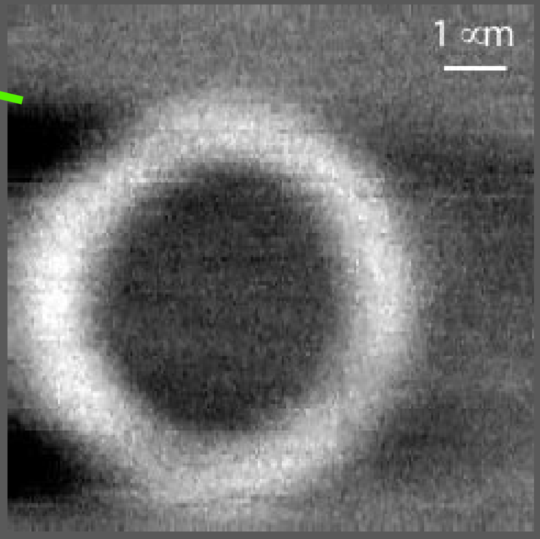

shows the amount of light that is absorbed/transmitted for different colors

e.g. fluorescent molecules

Atomic force microscopy

VOLUME 56, NUMBER 9 PHYSICAL REVIEW LETTERS 3 MARCH 1986

Atomic Force Microscope

G. Binnig[(a)] and C. F. Quate[(b)]
Edward L. Ginzton Laboratory, Stanford University, Stanford, California 94305

and

Ch. Gerber[(c)]
IBM San Jose Research Laboratory, San Jose, California 95193
(Received 5 December 1985)

As of 11/16/25: >8,800 citations

The Atomic Force Microscope

REVIEWS OF MODERN PHYSICS, VOLUME 75, JULY 2003

Advances in atomic force microscopy

Franz J. Giessibl*

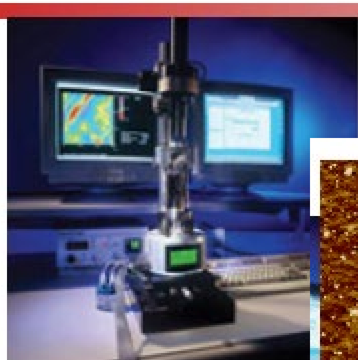

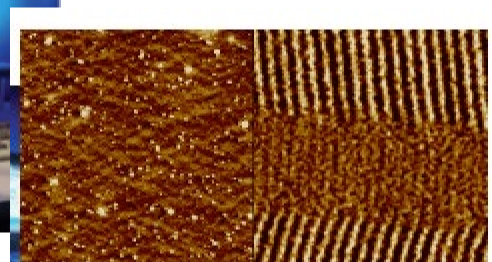

AFM MFM

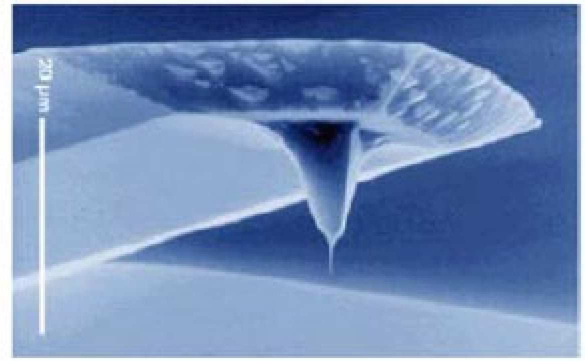

When Things work well

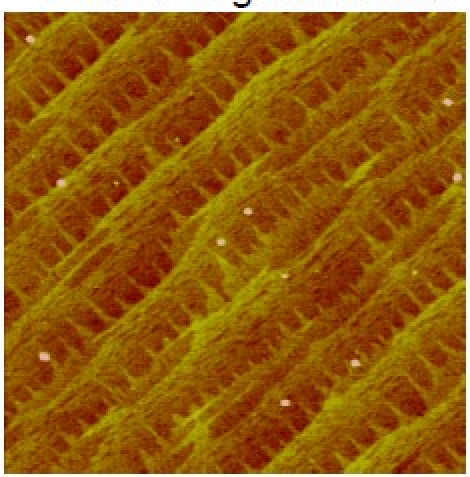

Typical Data

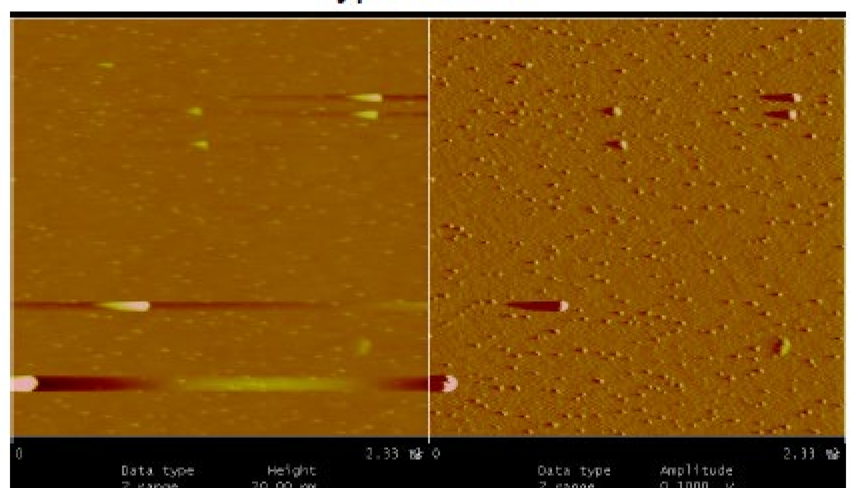

Atomic Force Microscope

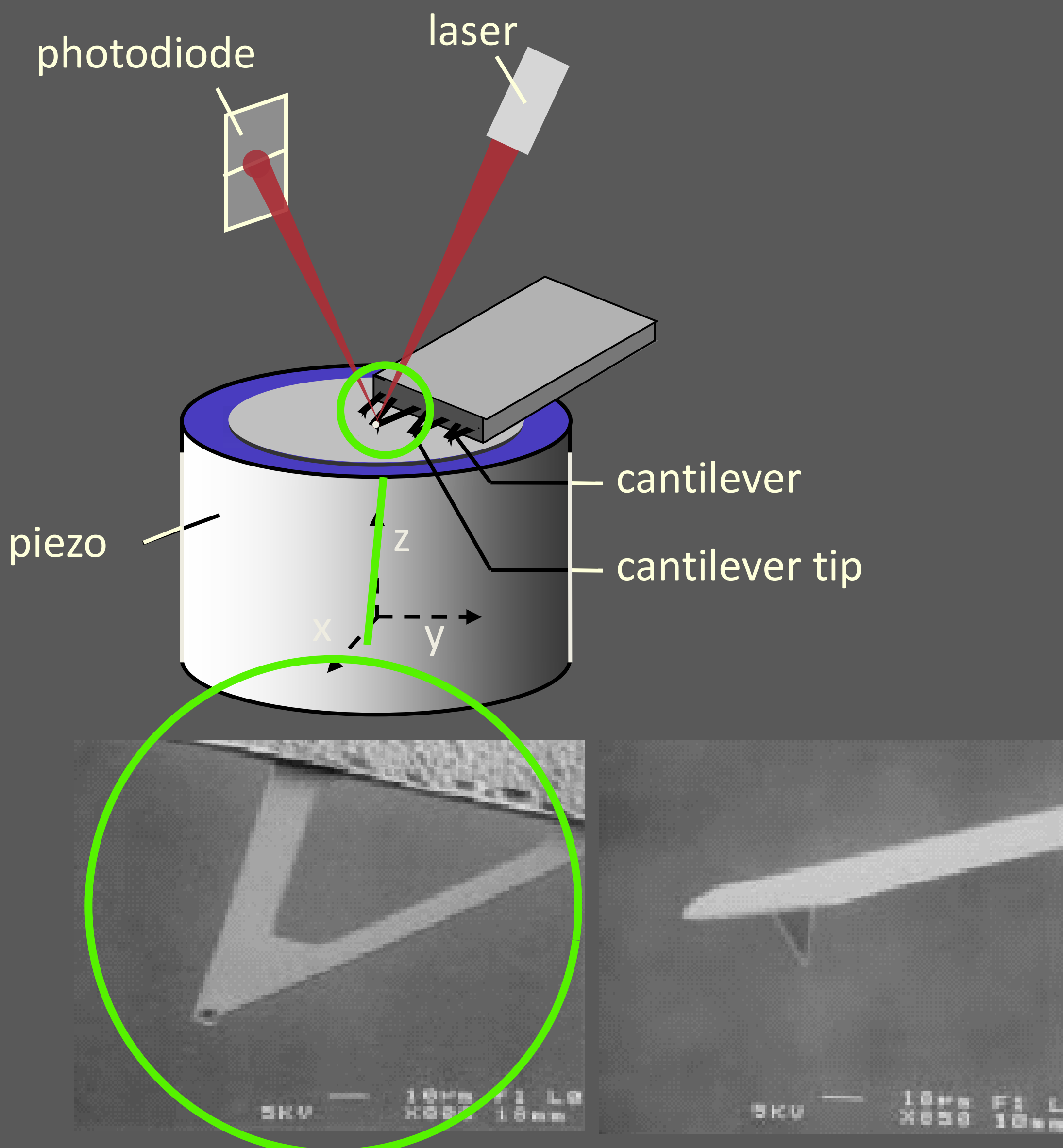

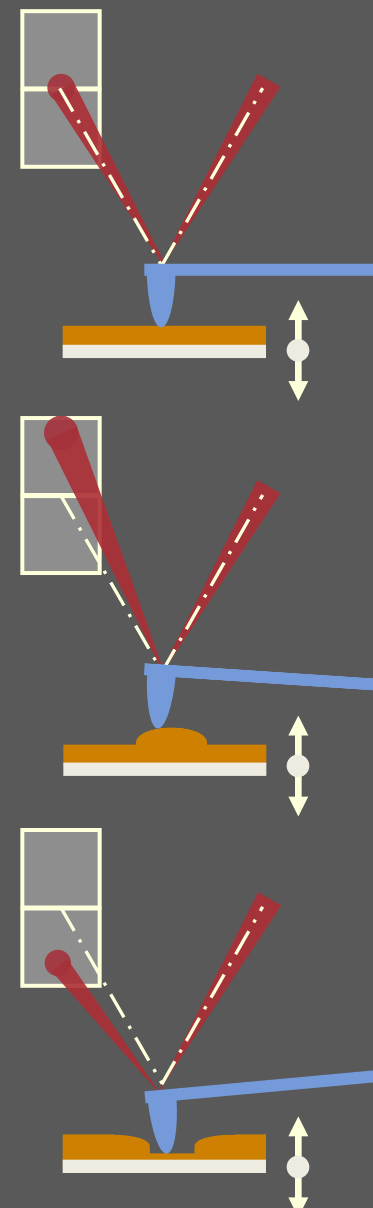

Atomic Force Microscope

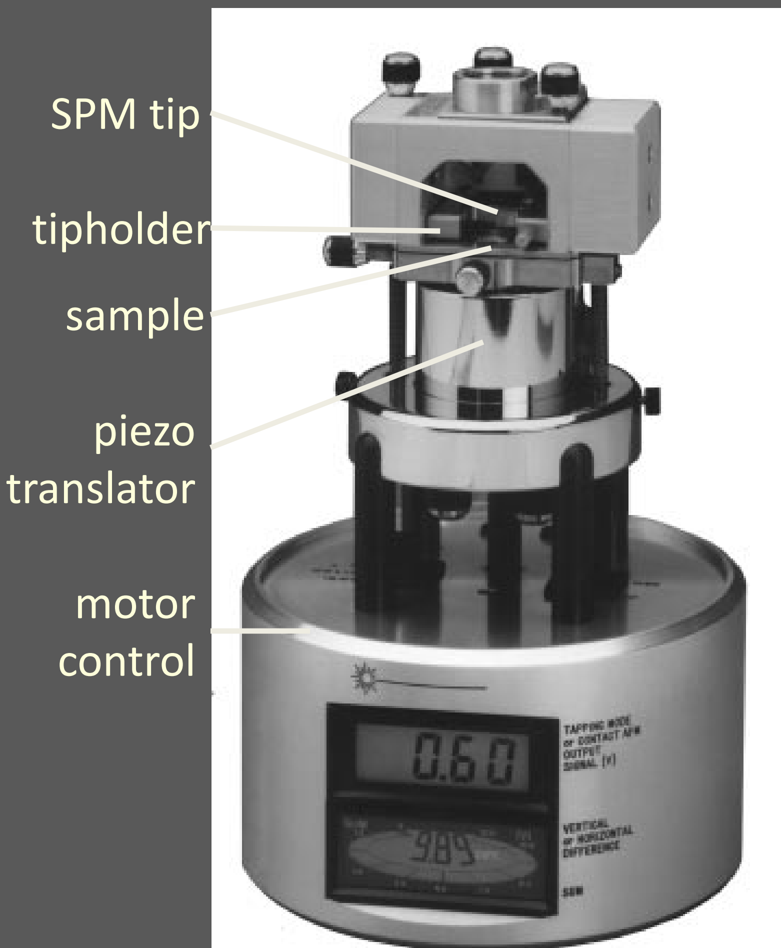

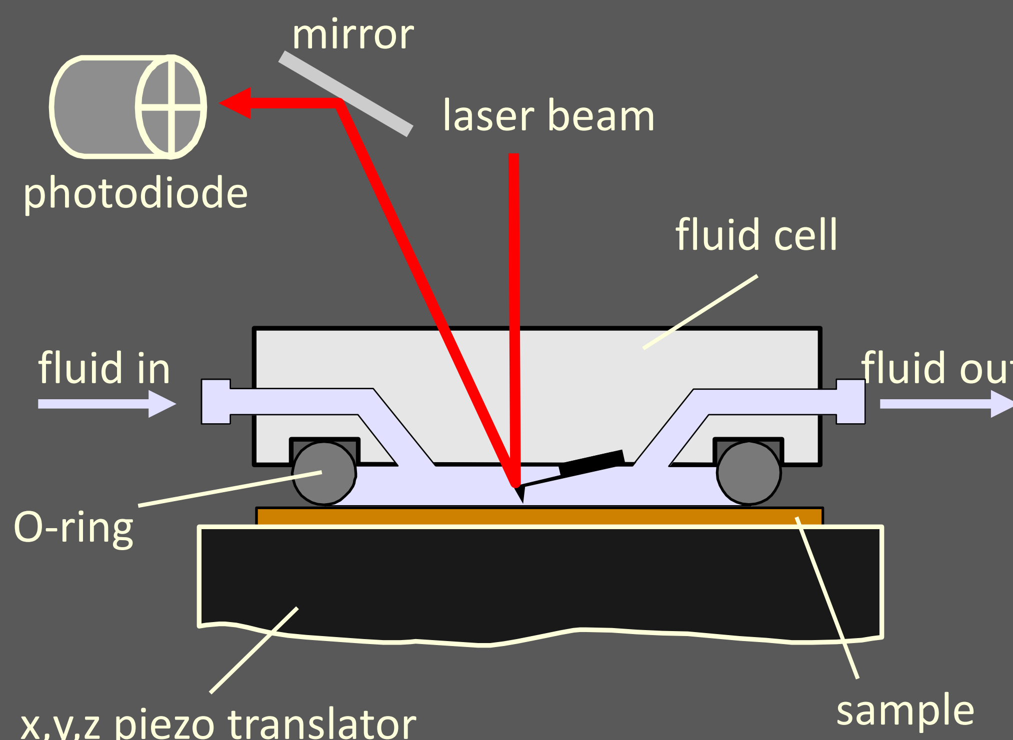

in air and in buffer solutions

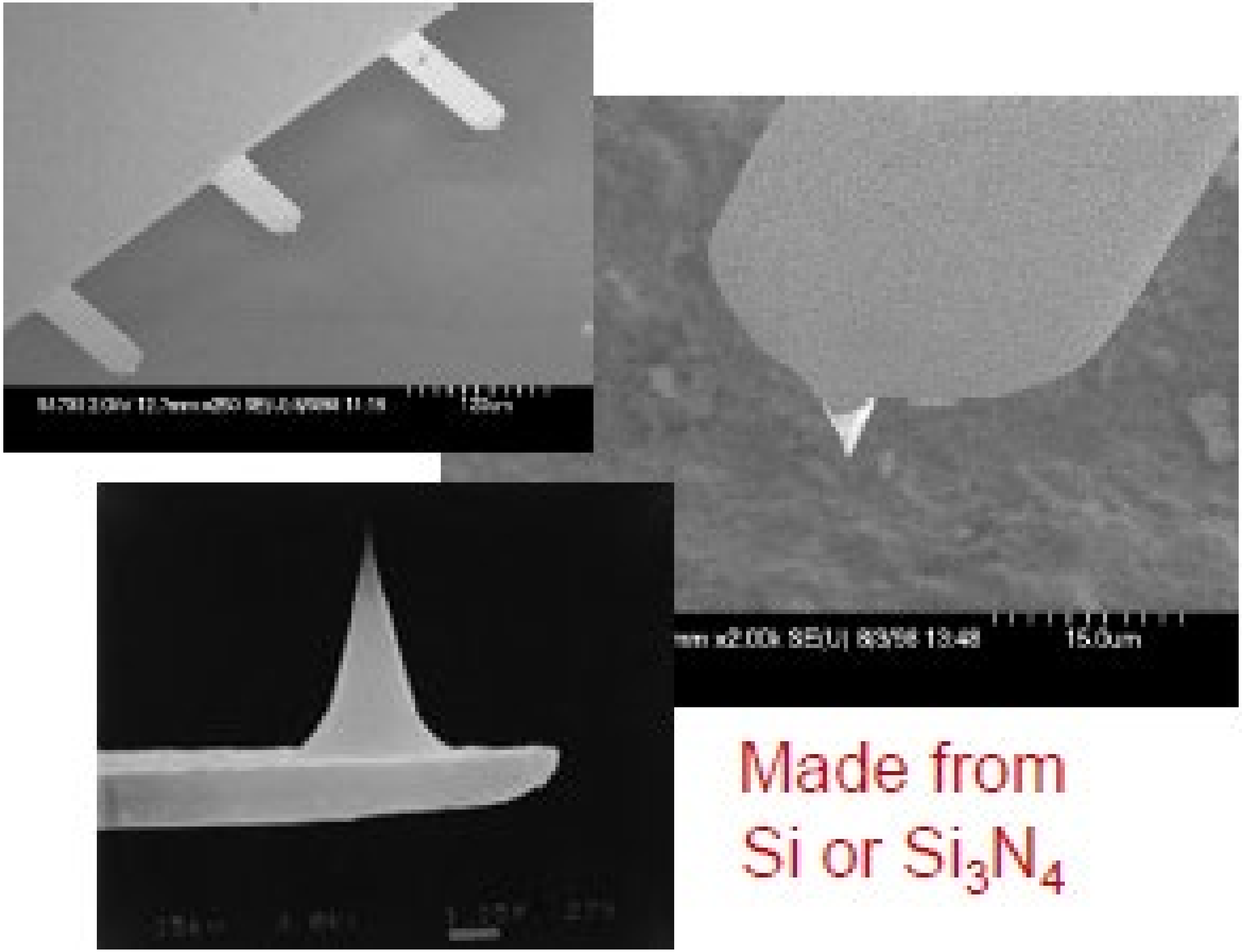

Made from Si or Si_3N_4

AFM Cantilever/Tip Styles

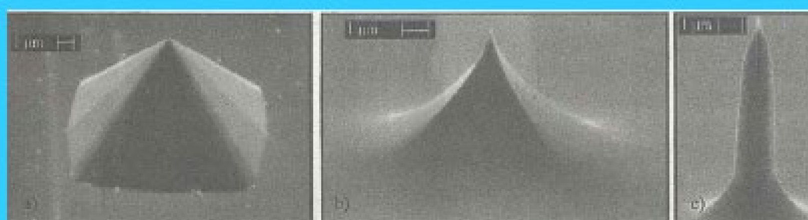

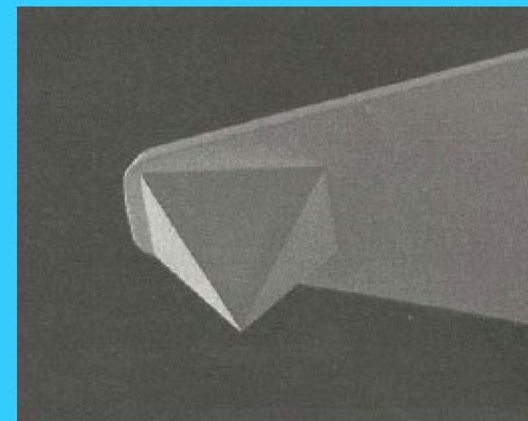

DNP Silicon Nitride Probes

- spring constants: 0.58, 0.32, 0.12, 0.06 N/m
- tip radius of curvature: 20-60nm
- cantilever length: 100 & 200μm
- reflective coating: gold
- shape of tip: square pyramidal
- tip half angle: 35°

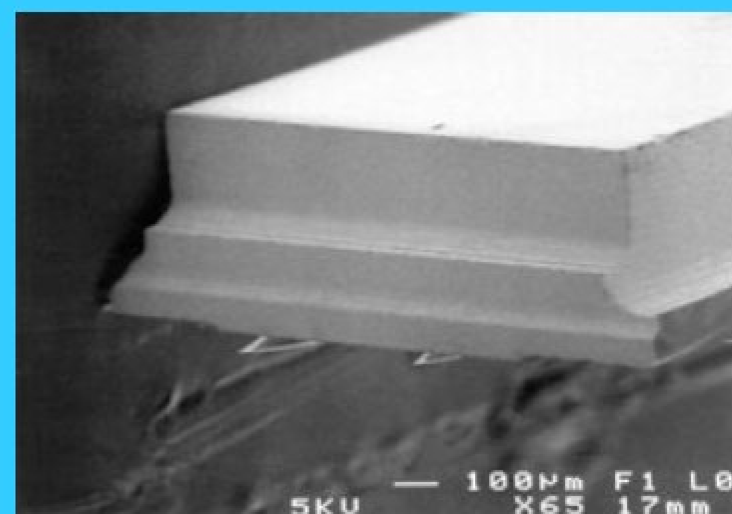

Tip Choices: A disposable supply

Silicon Nitride

- Contact Mode
- Soft enough to be deflected by small molecular forces

Silicon

- Tapping Mode
- Stiff for large force constant and resonance frequency

Silicon Nitride Probe Characteristics

Spring Constant (k)	0.58, 0.32, 0.12, 0.06 N/m [a]
Nominal Tip Radius of Curvature	20 - 60 nm
Cantilever Lengths	100 & 200 µm
Cantilever Configuration	V-shaped
Reflective Coating	Gold
Sidewall angles	35° on all 4 sides

a. Calculated spring constant values are based on the 0.6µm silicon nitride thickness; however, this value can actually vary from 0.4µm to 0.7µm. Thickness is cubed in the spring constant calculation, thus, actual values can vary substantially.

TappingMode Etched Silicon Probe (TESP) Characteristics

Spring Constant (k)	20 - 100 N/m
Resonant Frequency	200 - 400 kHz
Nominal Tip Radius of Curvature	5 - 10 nm
Cantilever Length	125 µm
Cantilever Configuration	Single Beam
Reflective Coating	Uncoated, Optional Al Coating

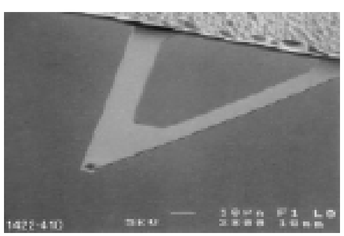

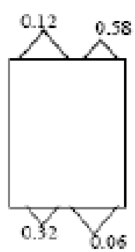

Four silicon nitri
tilevers showing
constants (N/m)

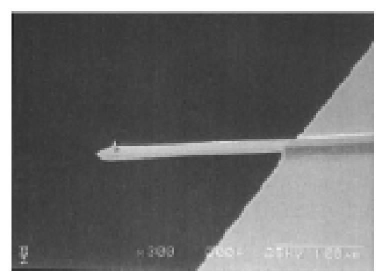

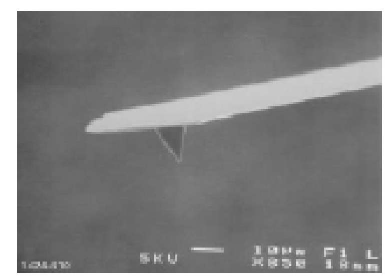

Atomic Forces Involved

Attractive and Repulsive Forces

- Pauli exclusion principle – no two electrons in an atom can be at the same time in the same state or configuration
- van der Waals Force – dipoles of individual particles
- Electrostatic or Coulombic Forces – ionic bonds
- Capillary and Adhesive Forces – liquid meniscus and tip contamination
- Double Layer Forces – ionic atmosphere around a charged substrate in fluid

AFM operating modes

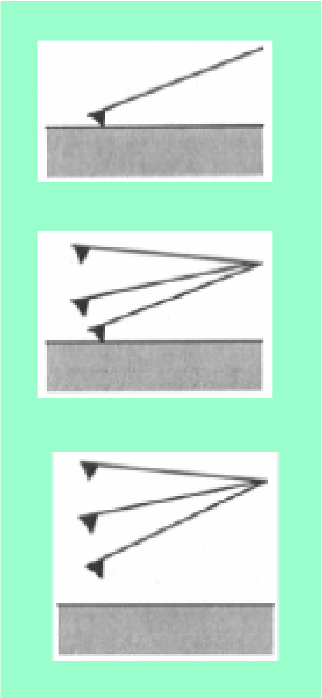

contact mode
C

Laser beam measures the deflection of the tip
Feedback to a piezoelectroc scanner keeps force (cantilever deflection) constant.

tapping mode
IC

Tip oscillates with the amplitude of several nm
Typical frequency 50 – 400 kHz
Touches the surface at the max. amplitude
Sample is moved up/down, so that amplitude is const.

non-contact mode
NC

Tip oscillates with the amplitude of several nm
Typica frequency 50 – 400 kHz
Remains 5-10 nm from the surface
Sample is moved up/down, so that amplitude is const.
Good for ”soft” materials

This is a very difficult mode to operate in ambient conditions with the AFM. The thin layer of water contamination which exists on the surface on the sample will invariably form a small capillary bridge between the tip and the sample and cause the tip to "jump-to-contact".

Contact mode

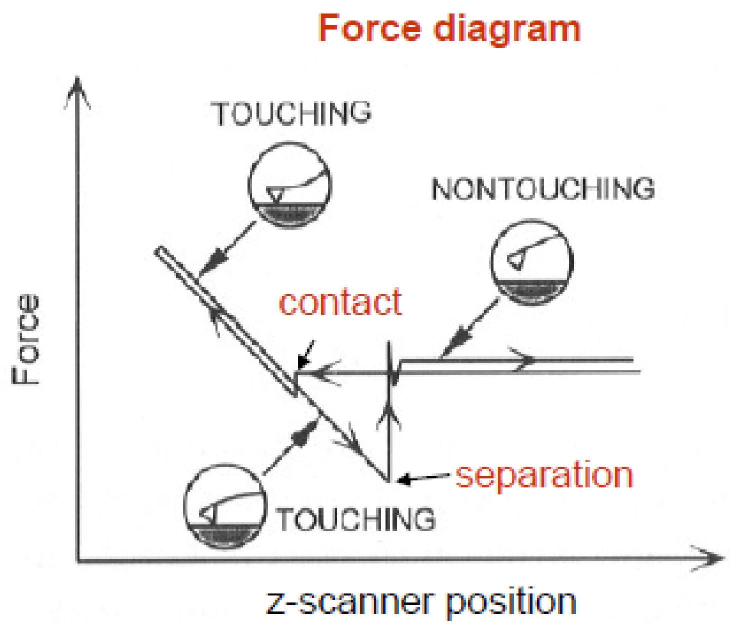

Practical problems:
- water or other liquid layer
- particles on surfaces
- electrical charging

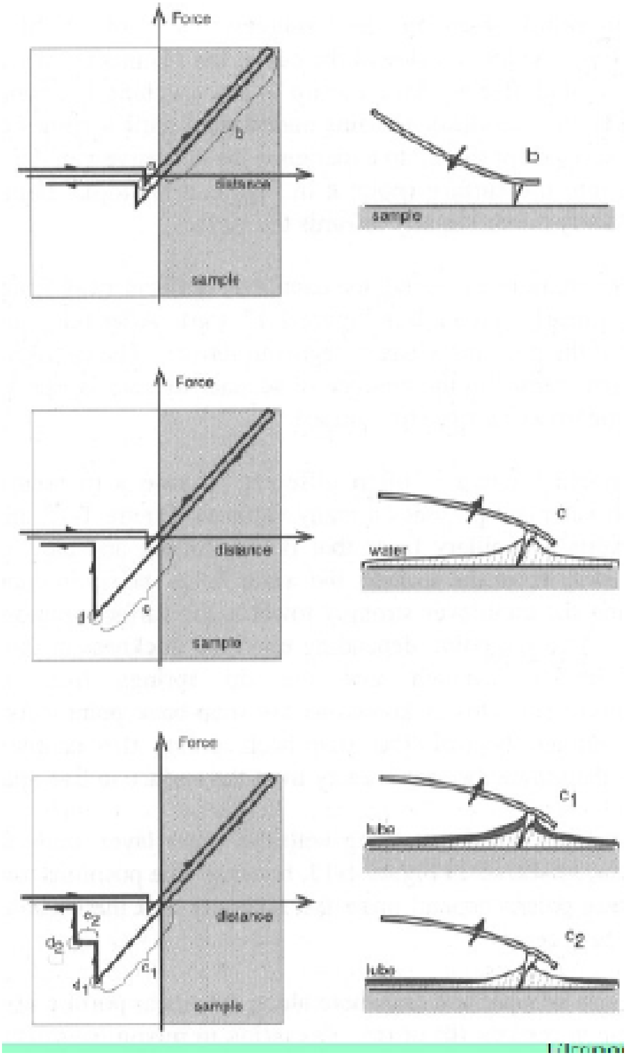

Contact mode

Advantages:

- High scan speed
- “Atomic resolution” images
- can scan rough samples with extreme changes in vertical topography

Disadvantages:

- Lateral (shear) forces can distort features
- capillary forces from the adsorbed fluid layer on the sample surface
- damage soft samples (polymers, biosamples, silicon) due to scraping

Lateral forces

The cantilever deformation (twisting) is elastic.
Horizontal force F_H is given by the Hooke's law:

$$\boxed{F_H = ks}$$

s – torsional deformation

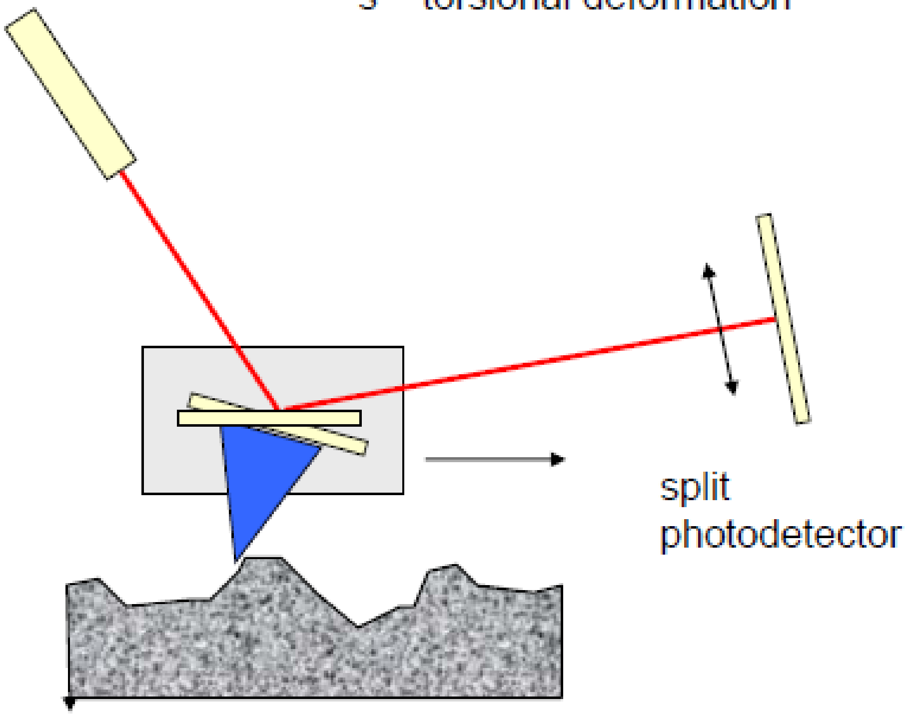

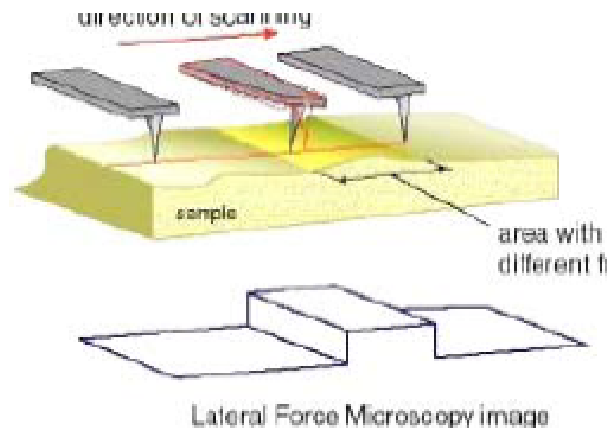

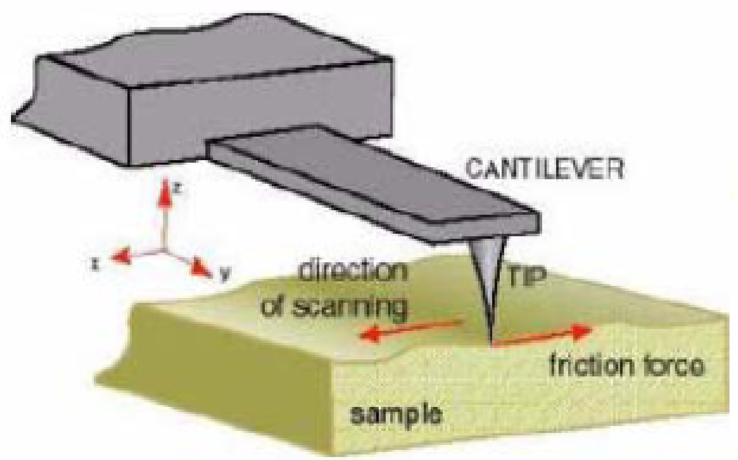

Lateral force Microscopy (LFM)

LFM measures the torsional deformation of the cantilever during scanning in contact mode.

The LFM image and topography can be obtained simultaneously. The lateral deformation depends on frictional (lateral) force acting on tip.

LFM studies are useful for imaging variations in surface friction that can arise from inhomogeneity in surface.

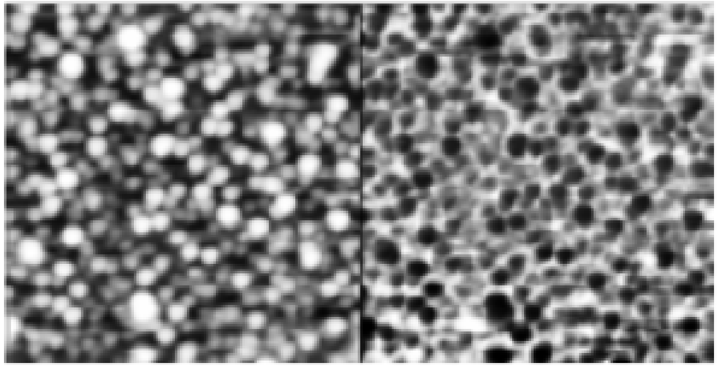

Friction force image of self assembled monolayers. Scale is 500 nm by 500 nm.

Left: Topographical (constant force) image
Right: Lateral force image

Tapping modes: frequency

Resonant oscillation frequency:

$$\boxed{\omega = \sqrt{\frac{k_{eff}}{m}}}$$

k_{eff}: effective force constant
m: cantilever mass

$$\boxed{k_{eff} = k - \Delta F}$$

k: force constant of cantilever
ΔF: change in the external force

movement

→ $\Delta F < 0$, k_{eff} increases, ω increases

← $\Delta F > 0$, k_{eff} decreases, ω decreases

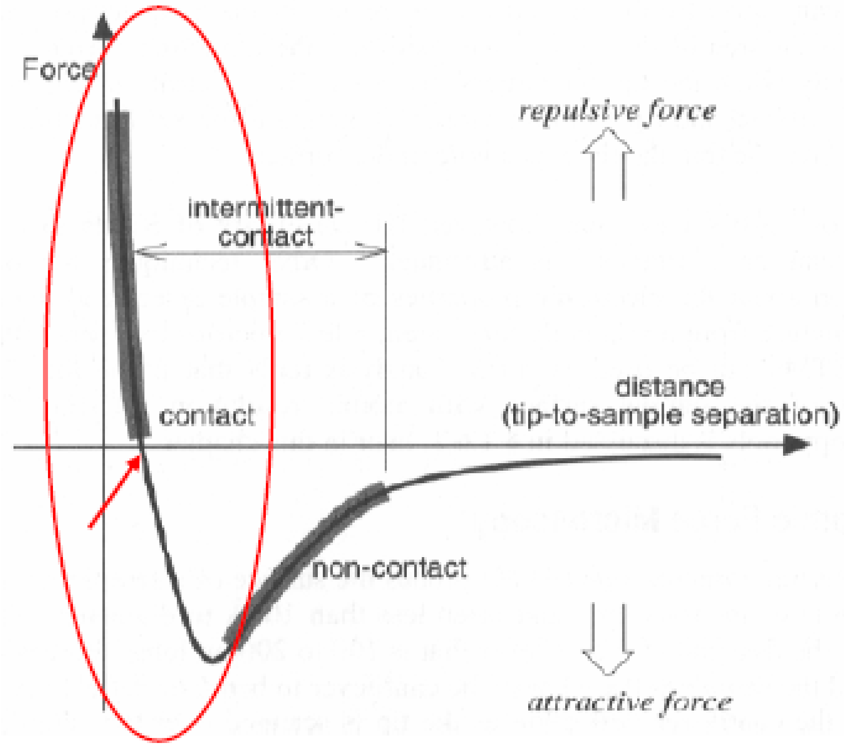

Noncontact vs. tapping mode

Tapping (IC) AFM:
- The oscillation frequency is selected smaller than the resonance frequency.
- When tip gets closer to the surface, resonance freq. becomes lower.
- Oscillation becomes more on-resonance ⇒ amplitude increases, tip is "pulled" to touch the surface
- Good if strong lateral forces between tip and surface – "dragging" or surface covered with liquid.

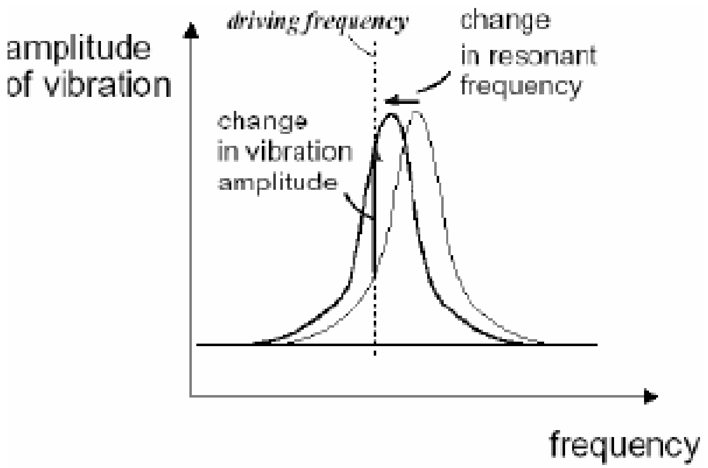

Noncontact (NC) AFM:
- The oscillation frequency is selected higher than the resonance frequency.
- When tip gets closer to the surface, resonance freq. becomes lower.
- Oscillation becomes more off-resonance ⇒ amplitude decreases.
- Feedback circuit tries to keep amplitude constant and removes tip away from surface.

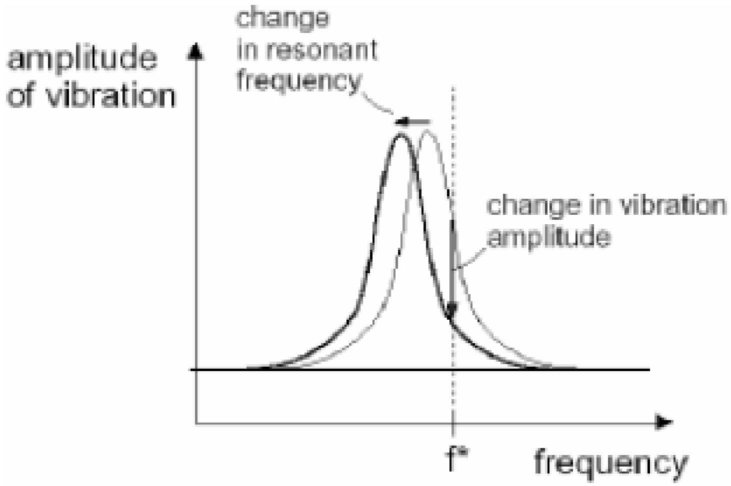

Figure 1-7. Response curves for a cantilever.

Tapping Mode

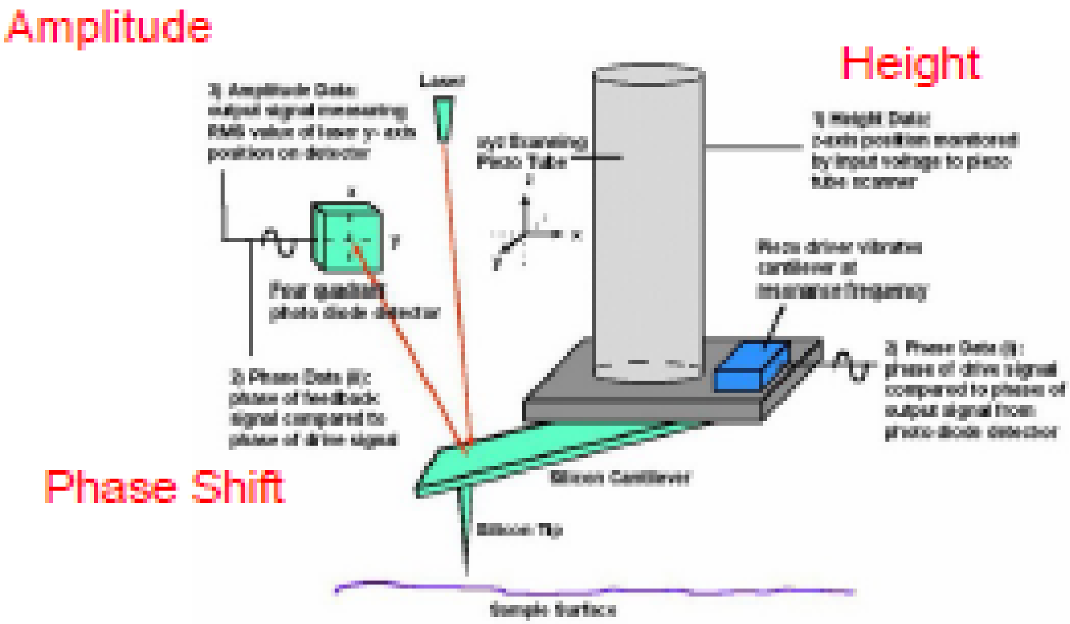

Disadvantages:

• slower scanning speed as compared to contact mode

Advantages:

• higher lateral resolution (1-5 nm)
• lower forces and less damage to soft samples imaged in air
• lateral forces are virtually eliminated; no scraping

Sidewall Measurements

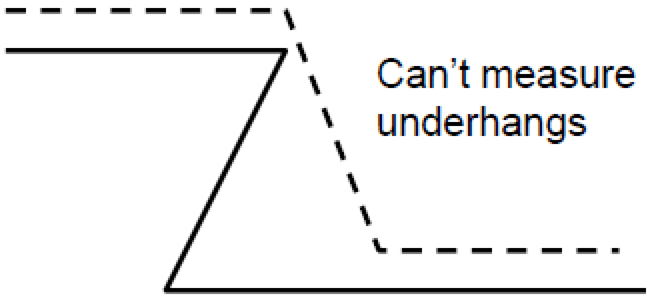

Can’t measure
underhangs

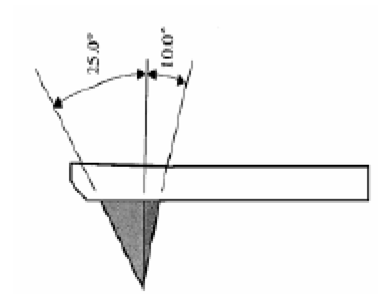

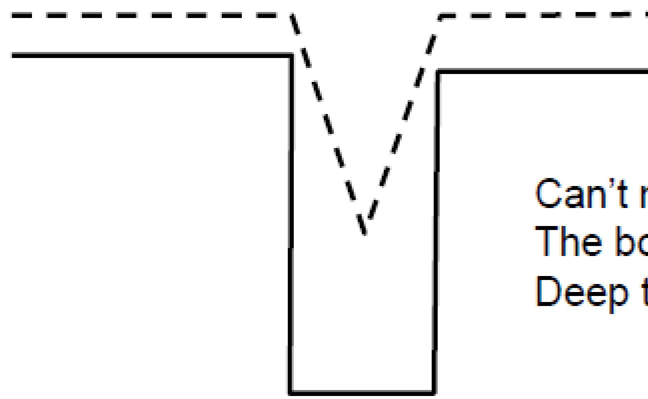

Can’t measure
The bottom of
Deep trenches

Imaging Artifacts: Broken or Blunt tip

All small features look the same
(and have the same orientation)

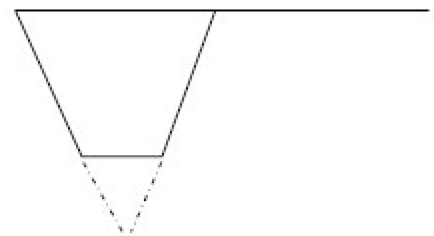

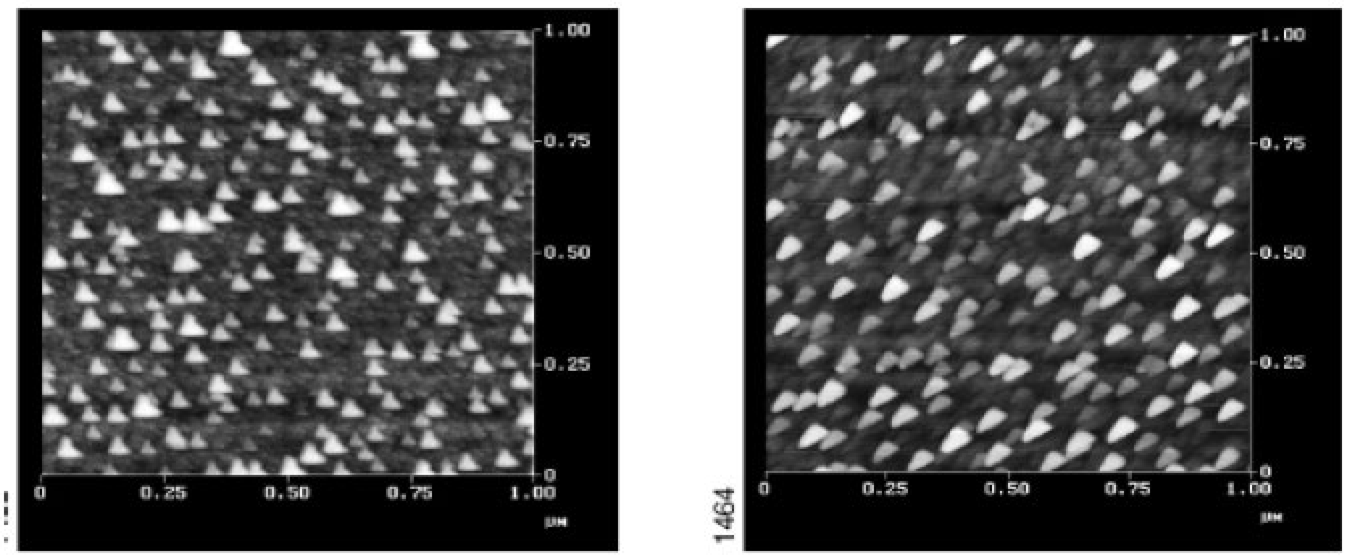

Figure 20.1 Dull or Dirty Tip
If the tip becomes worn or if debris attaches itself to the end of the tip, the features in the image may all have the same shape. What is really being imaged is the worn shape of the tip or the shape of the debris, not the morphology of the surface features.

Imaging Artifacts: Double Tip

All small features are doubled
(and have the same orientation)

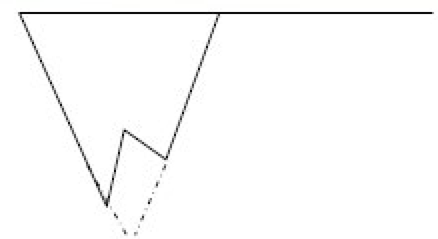

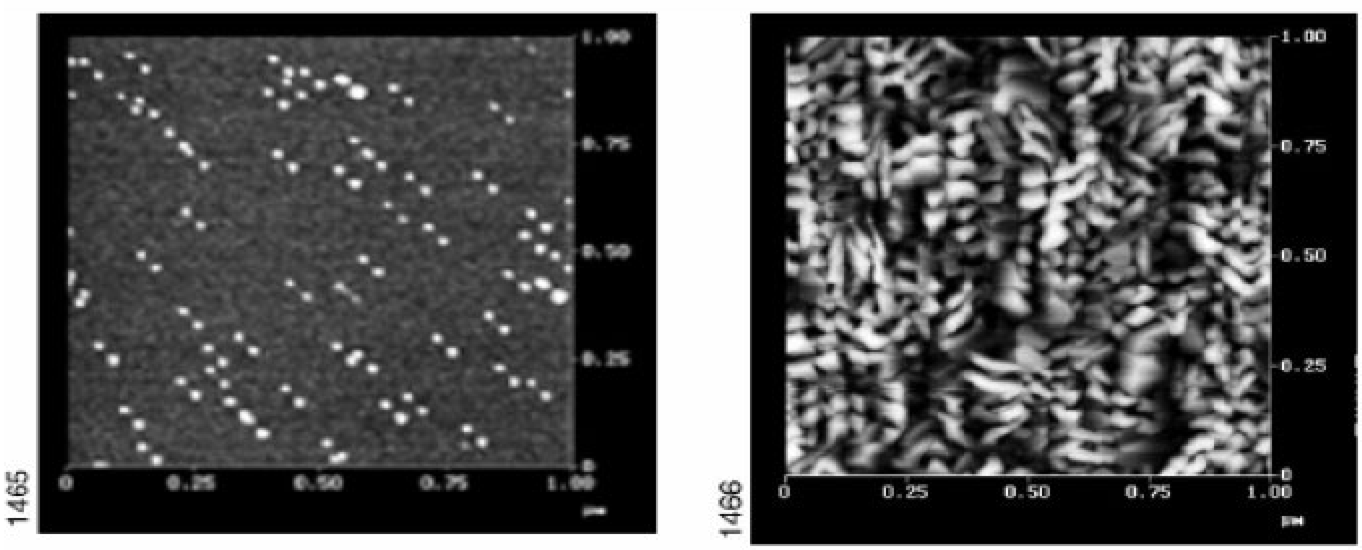

Figure 20.2 Double or Multiple Tips
Double or multiple tip images are formed with a tip with two or more end points which contact the sample while imaging. The above images are examples.

Imaging Artifacts: Contamination

Blurring or Streaking that
comes and goes

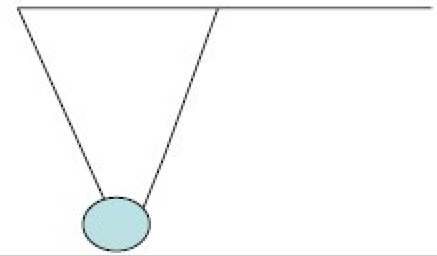

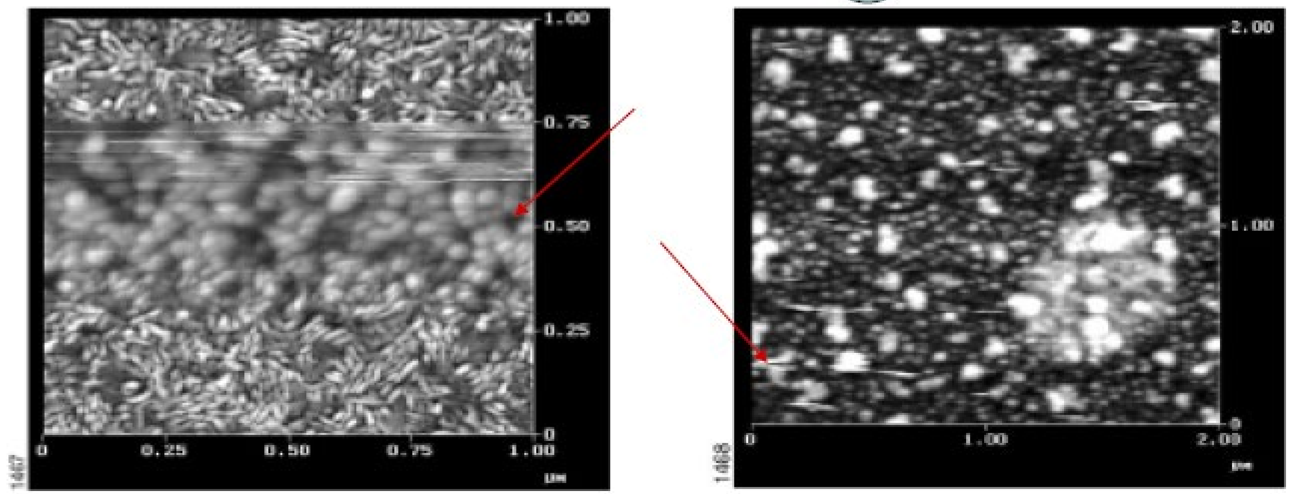

Figure 20.3 Contamination from Sample Surface
Loose debris on the sample surface can cause loss of image resolution and can produce streaking in the image. The image on the left is an example of the loss of resolution due to the build up of contamination on the tip when scanning from bottom-to-top. It can be seen how the small elongated features become represented as larger, rounded features until the debris detaches from the tip near the top of the scan. The image on the right is an example of skips and streaking caused by loose debris on the sample surface. Often, loose debris can be swept out of the image area after a few scans, making it possible to acquire a relatively clean image. Skips can also be removed from a captured image with the Erase Scan Lines function.

Imaging Artifacts: Optical Interference

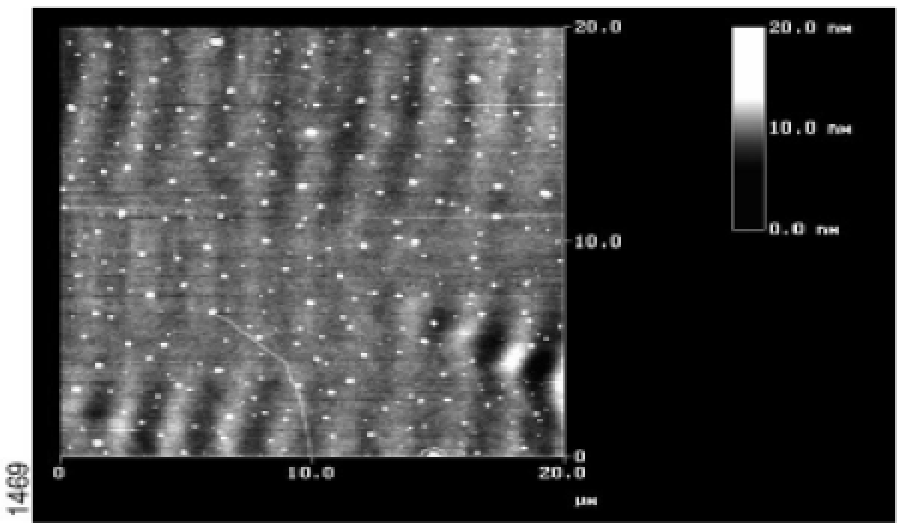

Figure 20.4 Optical Interference
Interference between the incident and reflected light from the sample surface can produce a sinusoidal pattern on the image with a period typically ranging between 1.5-2.5µm. This artifact is most often seen in contact mode on highly reflective surfaces, however, it occasionally appears in TappingMode. This artifact can usually be reduced or eliminated by adjusting the laser alignment so that more light reflects off the back of the cantilever and less light reflects off the sample surface.

spectrin

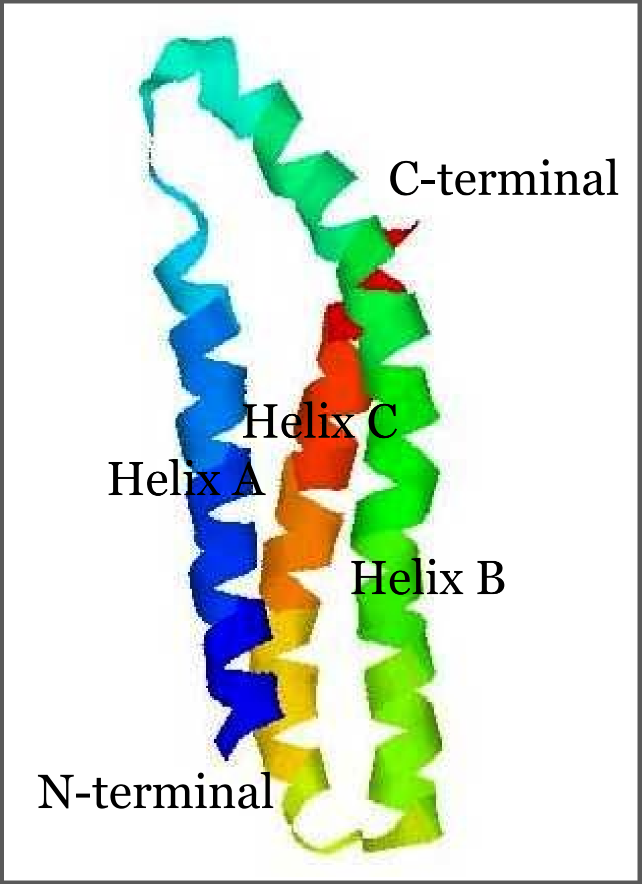

molecule that contributes to the mechanical properties, especially the elasticity of the cells

measurement of its mechanical stability provides information about the physiological function

Gerrit L. Heuvelman
Kirchhoff-Institut für Physik

stretching spectrin with an AFM

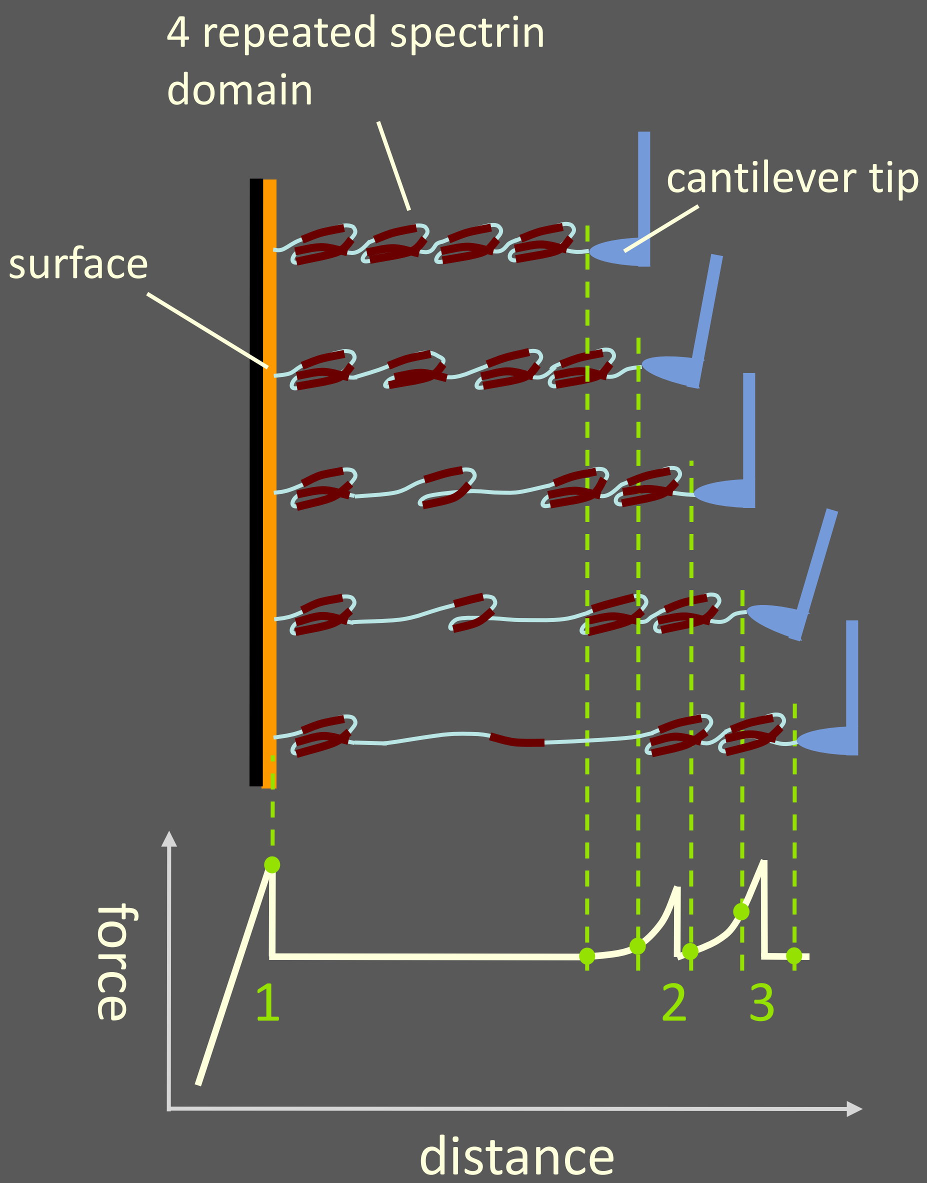

1. adhesion force between cantilever tip and surface

1. dissociation from the folded state to the intermediate unfolded state

1. dissociation from the intermediate to the total unfolding state

Gerrit L. Heuvelman
Kirchhoff-Institut für Physik

stretching spectrin with an AFM

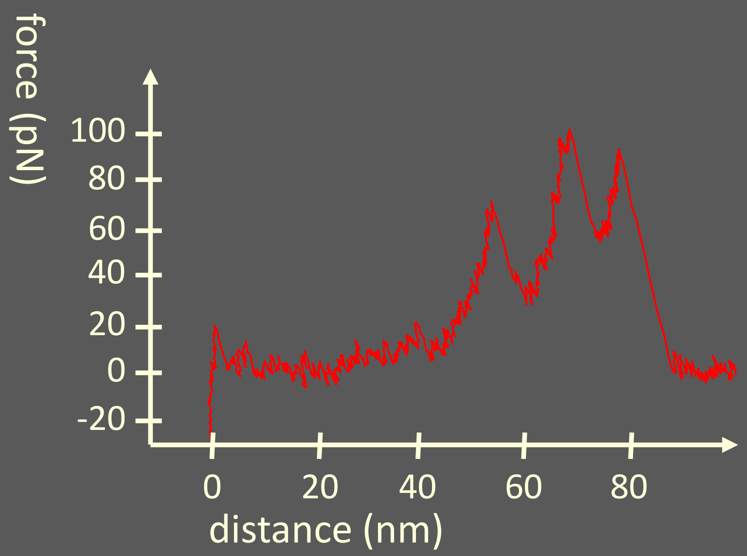

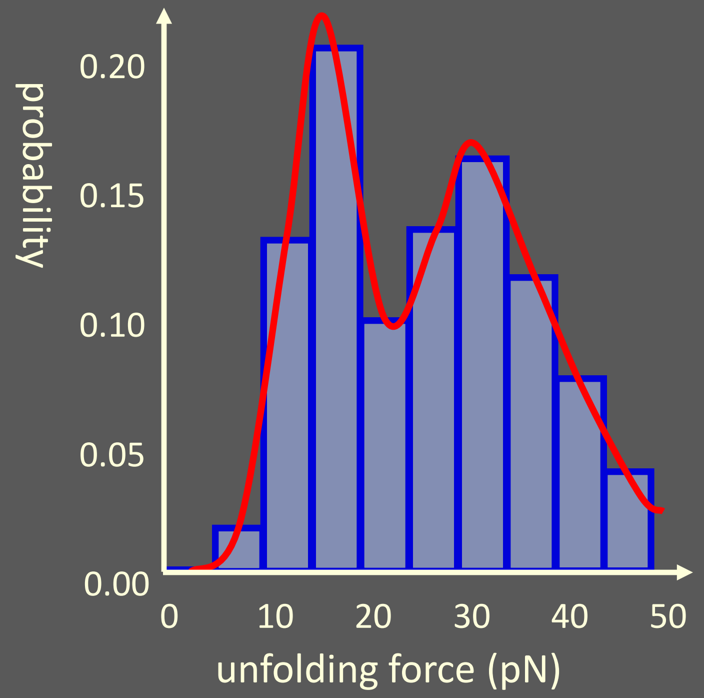

Gerrit L. Heuvelman

Kirchhoff-Institut für Physik

Vol 465 | 6 May 2010 | doi:10.1038/nature09024 nature

LETTERS

Designed biomaterials to mimic the mechanical properties of muscles

Shanshan Lv[1], Daniel M. Dudek[2]†, Yi Cao[1], M. M. Balamurali[1], John Gosline[2] & Hongbin Li[1]

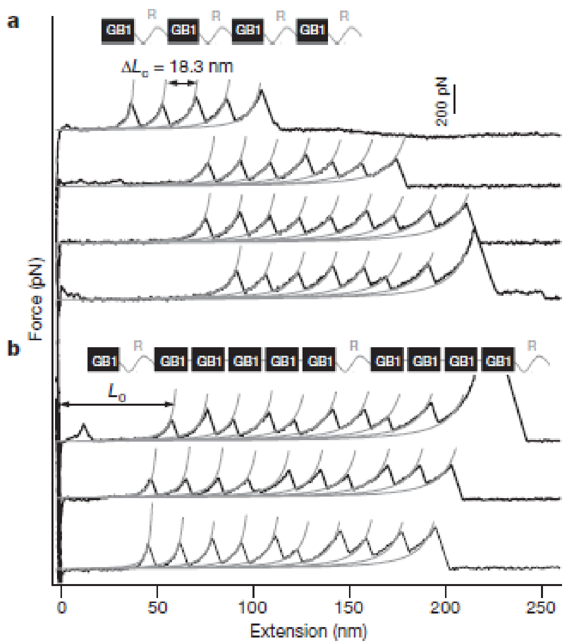

Figure 1 | Force–extension curves of two polyproteins. a, $(G–R)_4$. **b**, GRG_5RG_4R. The force peaks, characterized by a ΔL_c of ~18 nm and an unfolding force of ~180 pN, result from the mechanical unfolding of GB1 domains. Stretching resilins does not result in any unfolding force peaks; instead we see a featureless spacer of length L_0. The notable difference between the force–extension curves of $(G–R)_4$ and GRG_5RG_4R is the shorter featureless spacer of GRG_5RG_4R, which is due to fewer resilin repeats in GRG_5RG_4R. Grey lines correspond to the worm-like chain model fits to the experimental data.

a

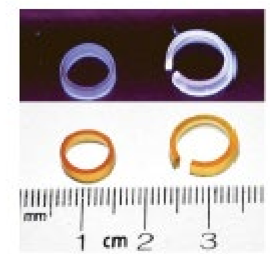

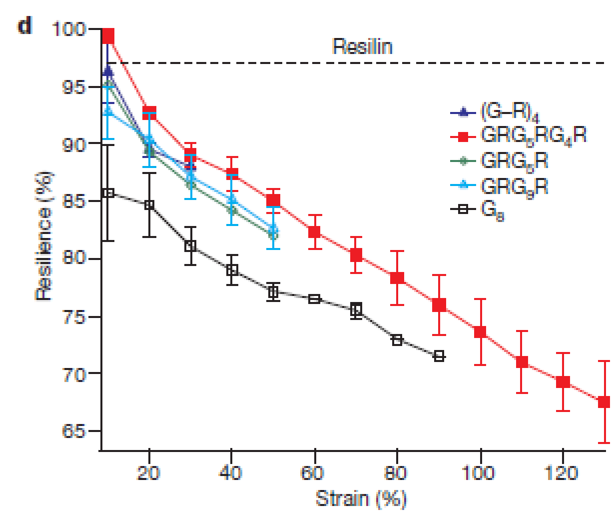

Science **337**, 1326 (2012);
DOI: 10.1126/science.1225621

Bond-Order Discrimination by Atomic Force Microscopy

Leo Gross,[1*] Fabian Mohn,[1] Nikolaj Moll,[1] Bruno Schuler,[1] Alejandro Criado,[2] Enrique Guitián,[2] Diego Peña,[2] André Gourdon,[3] Gerhard Meyer[1]

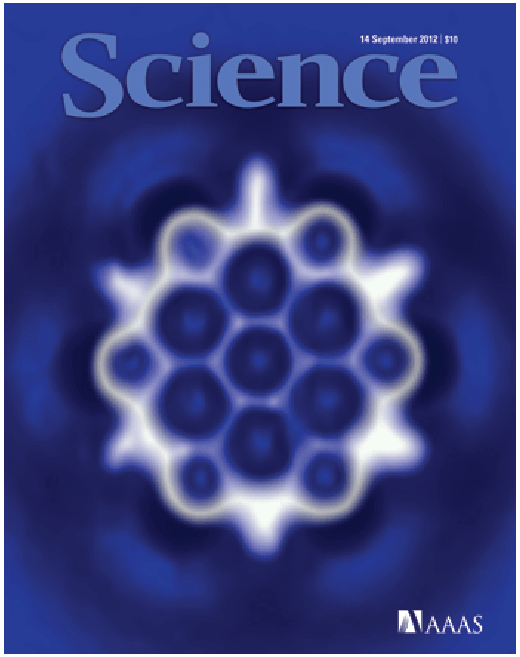

We show that the different bond orders of individual carbon-carbon bonds in polycyclic aromatic hydrocarbons and fullerenes can be distinguished by noncontact atomic force microscopy (AFM) with a carbon monoxide (CO)–functionalized tip. We found two different contrast mechanisms, which were corroborated by density functional theory calculations: The greater electron density in bonds of higher bond order led to a stronger Pauli repulsion, which enhanced the brightness of these bonds in high-resolution AFM images. The apparent bond length in the AFM images decreased with increasing bond order because of tilting of the CO molecule at the tip apex.

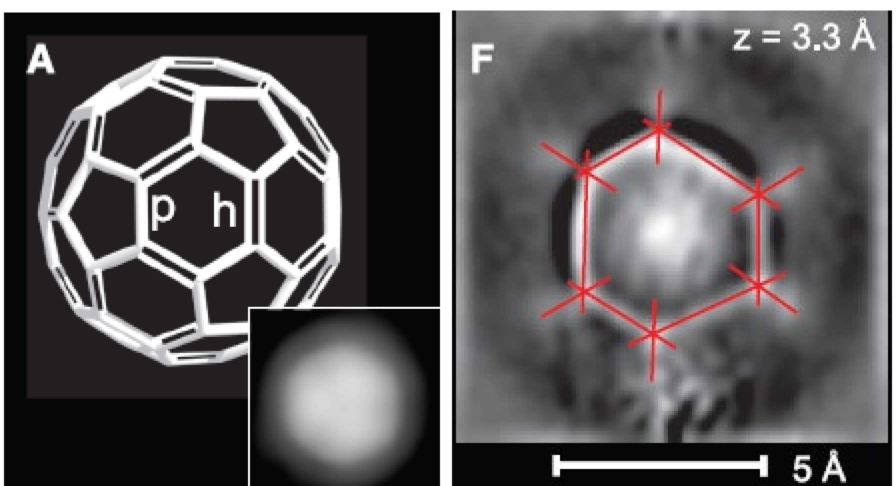

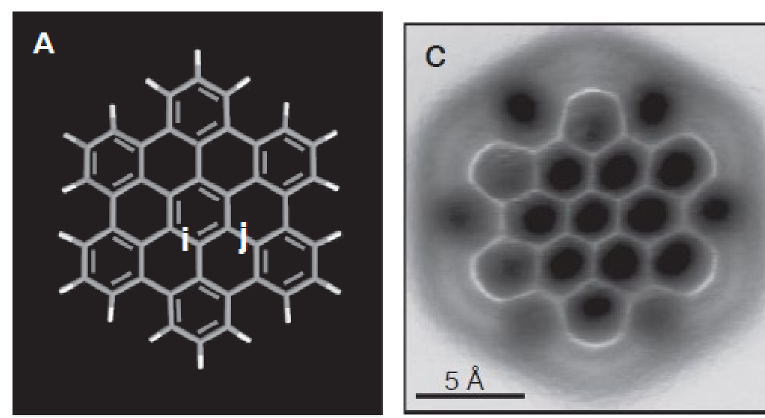

Electric force microscopy

- EFM is a is a secondary imaging mode derived from AFM.
- EFM measures electric field gradient distribution above the sample surface, through measuring local electrostatic interaction between a conductive tip and a sample .
- In EFM, a voltage is applied between the tip and the sample.
- The bias is used to create and modulate an electrostatic field between the tip and the substrate.
- The cantilever's resonance frequency and phase change with the strength of the electric field gradient and are used to construct the EFM image.
- EFM can be used to distinguish conductive and insulating regions in a sample.

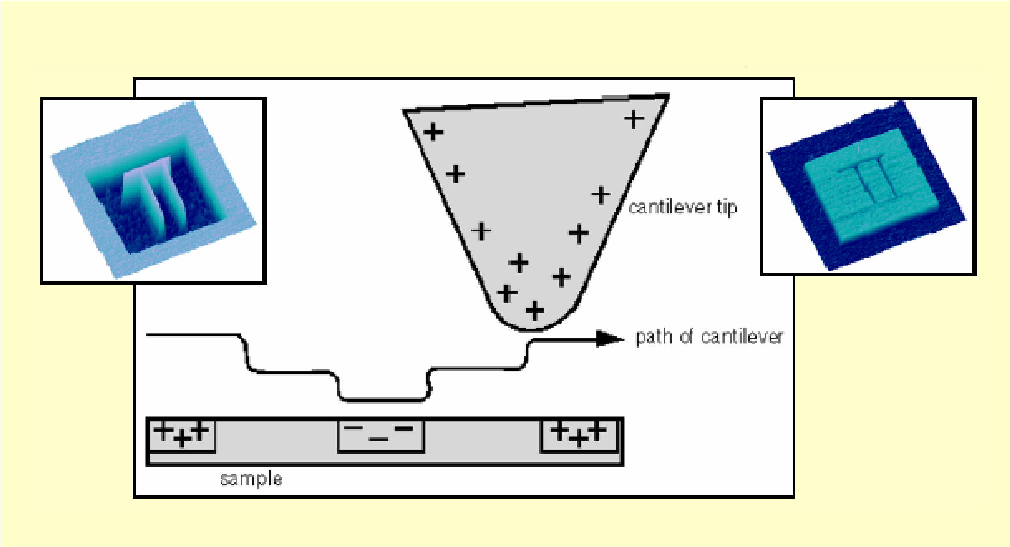

Typical applications of EFM

- characterizing surface electrical properties;
- electronic properties of nanocrystals (trap sites, charge storage, etc.);
- Interfacial charge transport and separation for organic/electrode devices (conducting polymer, organic semiconductors, etc.);
- detecting defects of an integrated circuit (silicon surface);
- measuring the distribution of a particular material on a composite surface;

VOLUME 93, NUMBER 11 PHYSICAL REVIEW LETTERS week ending 10 SEPTEMBER 2004

Microscopic View of Charge Injection in an Organic Semiconductor

William R. Silveira and John A. Marohn
Department of Chemistry and Chemical Biology, Cornell University, Ithaca, New York 14853-1301, USA
(Received 18 May 2004; published 10 September 2004)

We have measured the chemical potential and capacitance in a disordered organic semiconductor by electric force microscopy, following the electric field and interfacial charge density microscopically as the semiconductor undergoes a transition from Ohmic to space-charge limited conduction. Electric field and charge density at the metal-organic interface are inferred from the chemical potential and current. The charge density at this interface increases with electric field much faster than is predicted by the standard diffusion-limited thermionic emission theories.

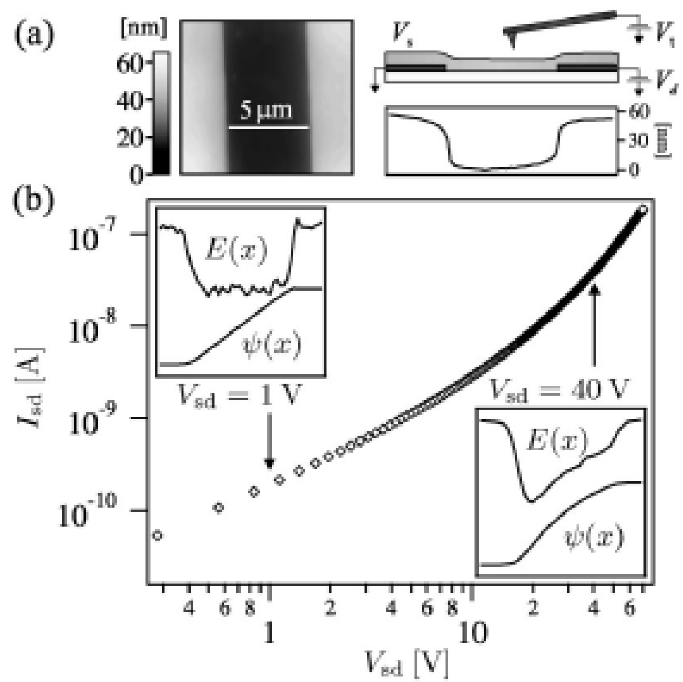

SCIENCE VOL 324 12 JUNE 2009

Measuring the Charge State of an Adatom with Noncontact Atomic Force Microscopy

Leo Gross,[1*] Fabian Mohn,[1] Peter Liljeroth,[1,2] Jascha Repp,[1,3] Franz J. Giessibl,[3] Gerhard Meyer[1]

Charge states of atoms can be investigated with scanning tunneling microscopy, but this method requires a conducting substrate. We investigated the charge-switching of individual adsorbed gold and silver atoms (adatoms) on ultrathin NaCl films on Cu(111) using a qPlus tuning fork atomic force microscope (AFM) operated at 5 kelvin with oscillation amplitudes in the subangstrom regime. Charging of a gold atom by one electron charge increases the force on the AFM tip by a few piconewtons. Moreover, the local contact potential difference is shifted depending on the sign of the charge and allows the discrimination of positively charged, neutral, and negatively charged atoms. The combination of single-electron charge sensitivity and atomic lateral resolution should foster investigations of molecular electronics, photonics, catalysis, and solar photoconversion.

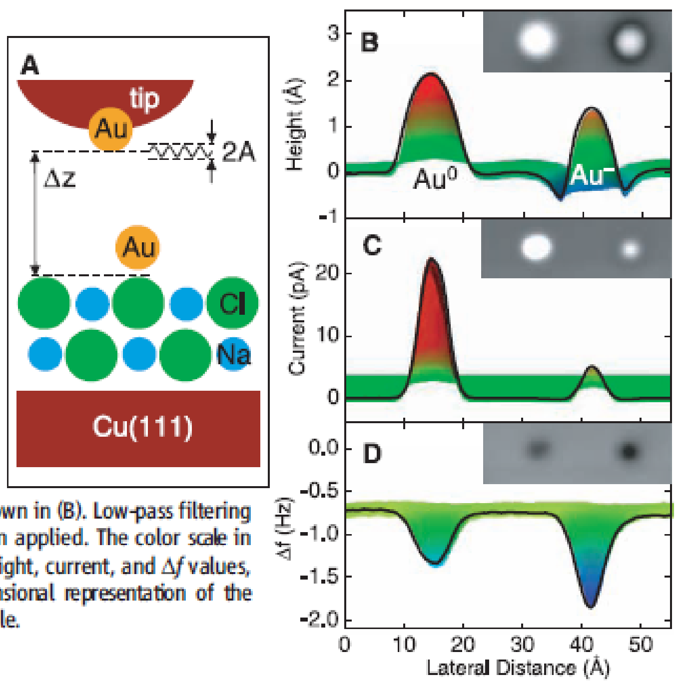

Fig. 1. (**A**) Model of the tip-sample geometry, showing the definition of the oscillation amplitude A and the tip height Δz (*26*). (**B**) Constant-current STM measurement [$V = -50$ mV and current (I) = 2 pA] of Au^0 (left) and Au^- (right) adsorbed on NaCl(2 ML)/Cu(111). The line scan is through the center of both atoms shown in the inset (image size of insets is 55 Å by 17 Å). (**C**) Current and (**D**) frequency shift recorded simultaneously in a constant-height measurement (Δz = 5.0 Å, $V = -5$ mV, and A = 0.3 Å) of the same area as shown in (B). Low-pass filtering (adjacent averaging) has been applied. The color scale in (B) to (D) corresponds to the height, current, and Δf values, respectively, in a three-dimensional representation of the images, cut along the line profile.

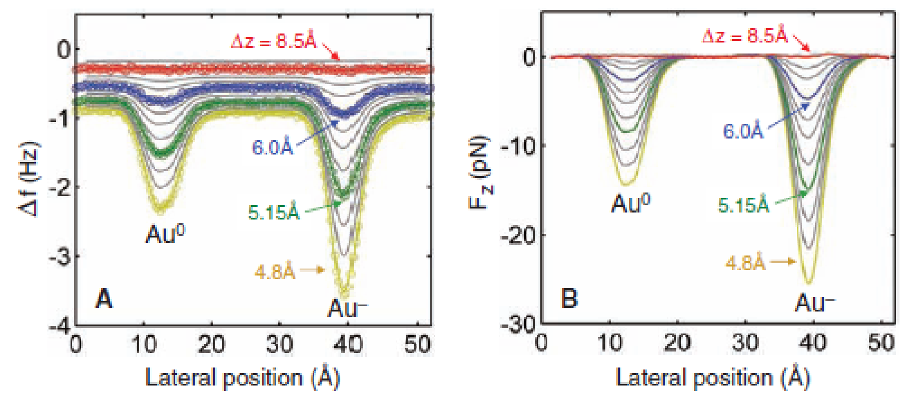

Fig. 2. (**A**) Frequency shift Δf recorded at a constant height (A = 0.22 Å and $V = -2$ mV) above Au^0 and Au^-. Different line scans correspond to different tip heights Δz as indicated. For some curves, every eighth point of the raw data are shown as an open circle in Fig. 2A; the solid lines correspond to the averaged data. (**B**) Vertical force F_Z^* extracted from the averaged data in (A) with the oscillation amplitude deconvolved and the constant background force subtracted from each curve (*26*).

Scanning tunneling microscopy

Scanning Tunneling Microscopy
Measures $|\Psi(x,E)|^2$

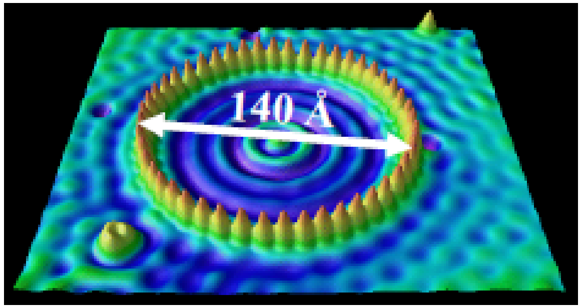

Fe on Cu

Crommie, *et al.*, Science **262**, 218 (1993).

Atom Manipulation - Don Eigler IBM

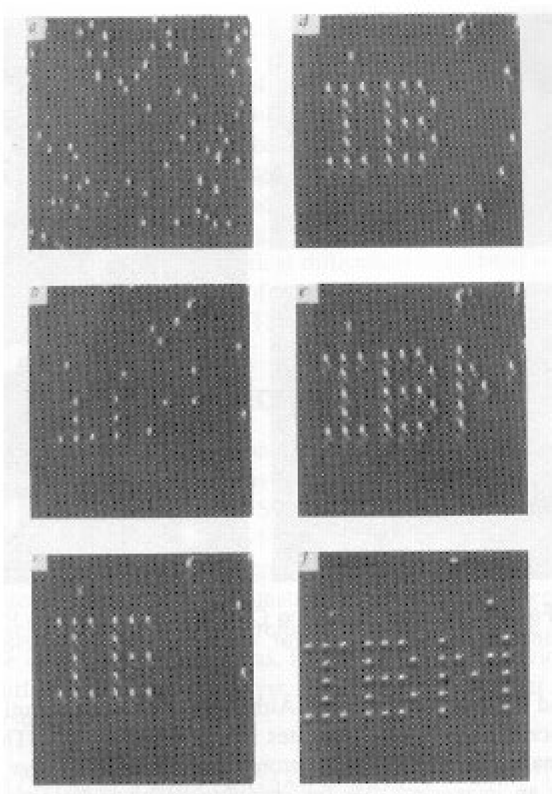

Xe atoms on Ni(100) at 8 K assembled by tip manipulation to spell "IBM". 1989

Quantum mechanical electron "standing waves" change the STM Tunnel Current

Fe atoms arranged by STM manipulation

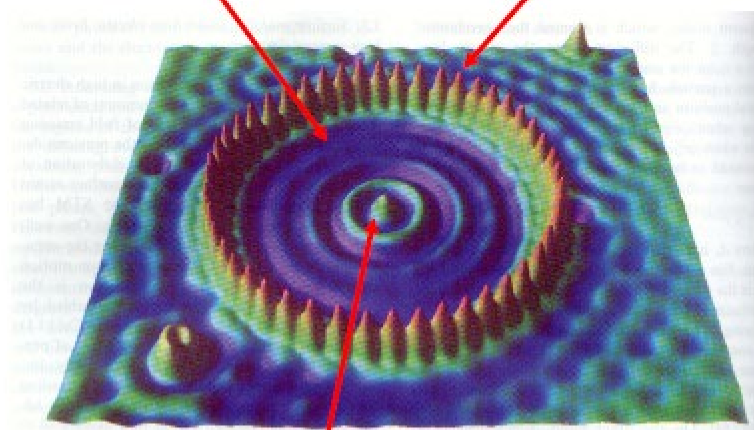

Fig. 9. An STM image of the quantum corral, consisting of 48 iron atoms on Cu(111). The image size is 200 × 200 nm^2 [89] (courtesy of IBM Almaden Research Center).

A node in the electron standing wave pattern (not an atom)

***Title** : The Beginning*

***Media** : Xenon on Nickel (110)*

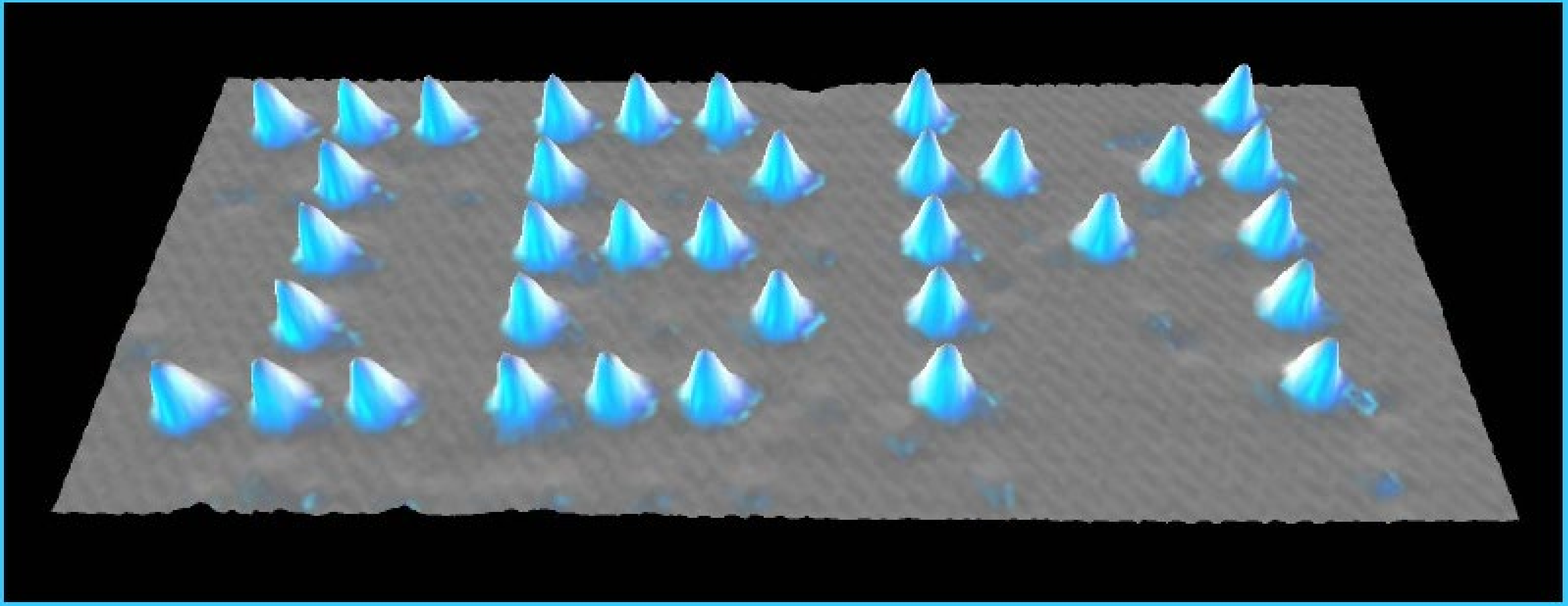

D.M. Eigler, E.K. Schweizer. Positioning single atoms with a scanning tunneling microscope. ***Nature 344, 524-526 (1990).***

STM: experiment

VOLUME 50, NUMBER 2 PHYSICAL REVIEW LETTERS 10 JANUARY 1983

7 × 7 Reconstruction on Si(111) Resolved in Real Space

G. Binnig, H. Rohrer, Ch. Gerber, and E. Weibel
IBM Zurich Research Laboratory, 8803 Rüschlikon-ZH, Switzerland
(Received 17 November 1982)

The 7×7 reconstruction on Si(111) was observed in real space by scanning tunneling microscopy. The experiment strongly favors a modified adatom model with 12 adatoms per unit cell and an inhomogeneously relaxed underlying top layer.

Si(111)

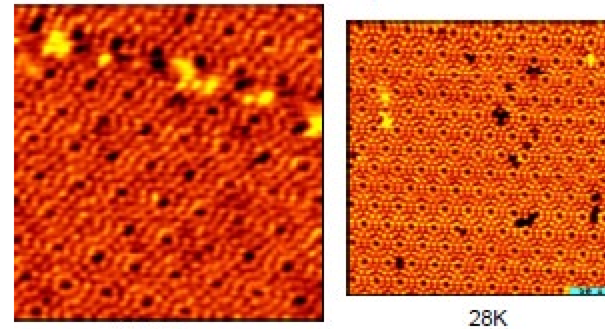

1000K 28K

1.2nm CNT

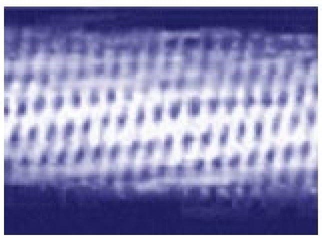

STM: theory

VOLUME 6, NUMBER 2 PHYSICAL REVIEW LETTERS JANUARY 15, 1961

TUNNELLING FROM A MANY-PARTICLE POINT OF VIEW*

J. Bardeen
University of Illinois, Urbana, Illinois
(Received December 16, 1960)

VOLUME 50, NUMBER 25 PHYSICAL REVIEW LETTERS 20 JUNE 1983

Theory and Application for the Scanning Tunneling Microscope

J. Tersoff and D. R. Hamann
Bell Laboratories, Murray Hill, New Jersey 07974
(Received 17 March 1983)

Why STM Works: Tunneling Current is exponential in Distance

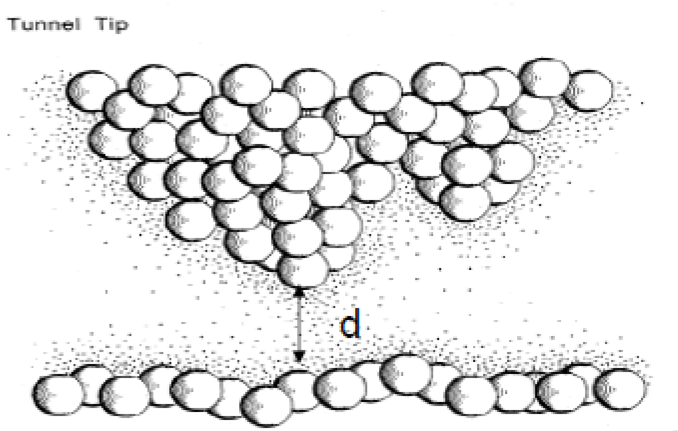

Binning and Rohrer, *Rev Mod Phys* **59** 615 (1987)

$$I \,\alpha\, \exp(-2\chi d)$$

$$\chi = \sqrt{\frac{2m}{\hbar^2}\phi}$$

For ϕ~ 4 eV, χ ~ 1Å^{-1}

Signal drops by order of magnitude/A

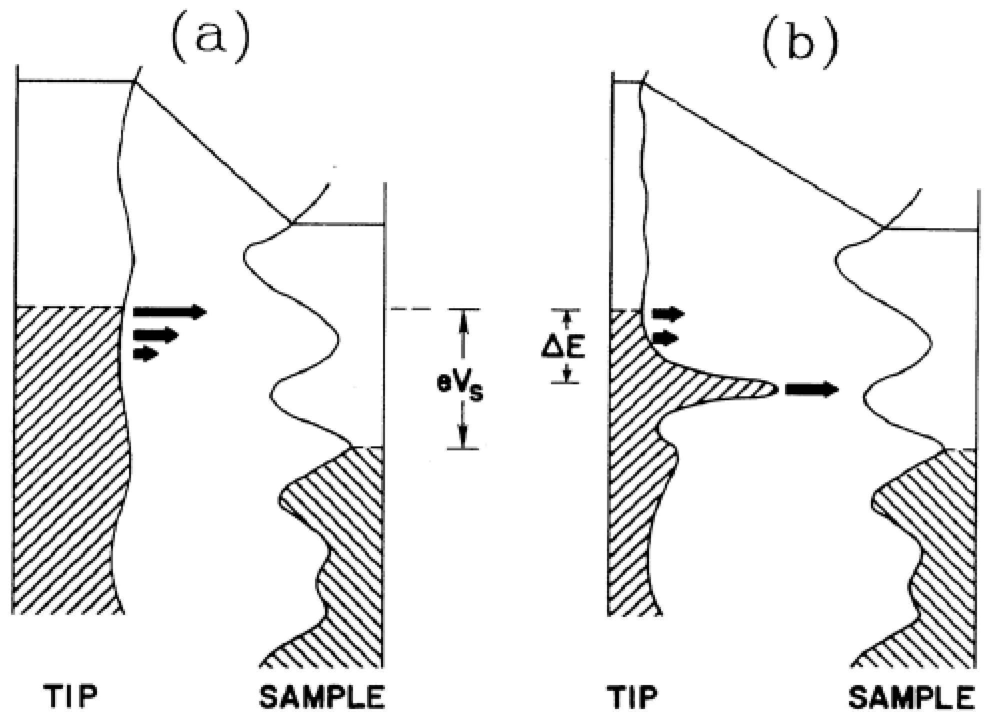

FIG. 5. Schematic energy-level diagrams for a sample and (a) a uniform tip, (b) a nonuniform tip with filled peak at energy ΔE below Fermi level. Arrows represent electron-tunneling probability at a given energy.

Pelz, PRB **43**, 6746 (1991)

Scanning Tunneling Microscopy of Graphite

S. Hembacher, F. Giessibl, J. Mannhart, and . F. Quate, Proc. Nat. Acad. Sci, **100** 12539 (2003)

STM AFM

Expt

Theory

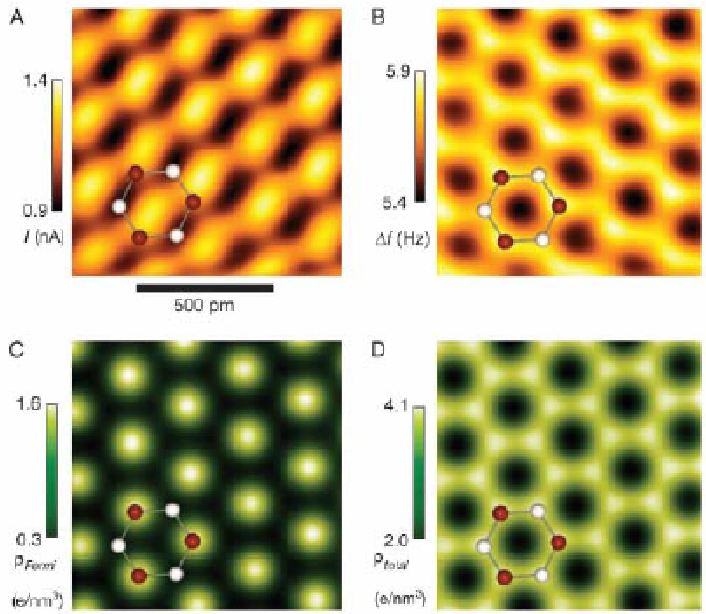

Fig. 3. Experimental and simulated STM and AFM images of graphite. One hexagonal surface unit cell with the two basis atoms α (white) and β (red) is superimposed for clarity. (*A*) Experimental image of graphite in constant-height dynamic STM mode (bias voltage +100 mV, amplitude 300 pm, scanning speed 0.2 nm/s). The tunneling current ranges from 0.9 to 1.4 nA. Only the β atoms appear in the image. The green arrow indicates a shift of the experimental STM image with respect to the AFM image by 68 pm (see text). (*B*) Experimental image of graphite in constant-height dynamic AFM mode showing both α and β atoms. The frequency shift data have been recorded simultaneously with the tunneling data shown in *A*, ranging from +5.4 to +5.9 Hz. (*C*) The calculated charge density of graphite at the Fermi level ρ_{Fermi} (after refs. 11 and 12) at a height of 200 pm over the surface plane, ranging from 0.3 to 1.6 electrons per nm^3. The maxima of ρ_{Fermi} are at the β atom positions. The STM image reflects the charge density at the Fermi level. (*D*) Calculated total charge density, also at a height of 200 pm over the surface plane, ranging from 2.0 to 4.1 electrons per nm^3. The repulsive forces that are imaged in the experimental AFM image (*B*) are increasing with the charge density; thus, a charge density plot is a good approximation for a repulsive AFM image. The experimental image in *B* and the calculated charge density shown in *D* have local maxima over α and β sites.

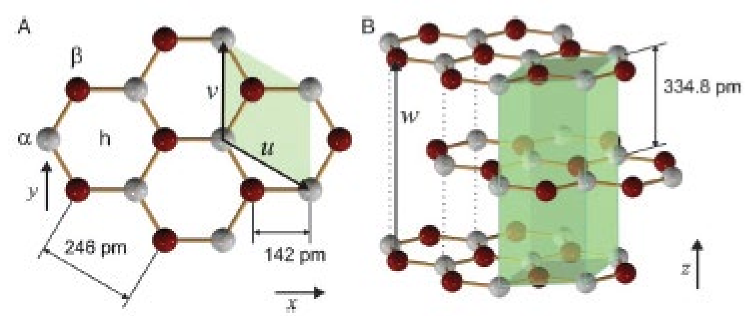

SCIENCE VOL 317 13 JULY 2007

Scattering and Interference in Epitaxial Graphene

G. M. Rutter,[1] J. N. Crain,[2] N. P. Guisinger,[2] T. Li,[1] P. N. First,[1*] J. A. Stroscio[2*]

A single sheet of carbon, graphene, exhibits unexpected electronic properties that arise from quantum state symmetries, which restrict the scattering of its charge carriers. Understanding the role of defects in the transport properties of graphene is central to realizing future electronics based on carbon. Scanning tunneling spectroscopy was used to measure quasiparticle interference patterns in epitaxial graphene grown on SiC(0001). Energy-resolved maps of the local density of states reveal modulations on two different length scales, reflecting both intravalley and intervalley scattering. Although such scattering in graphene can be suppressed because of the symmetries of the Dirac quasiparticles, we show that, when its source is atomic-scale lattice defects, wave functions of different symmetries can mix.

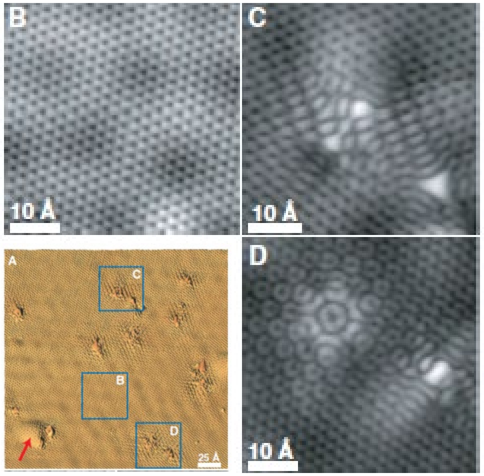

Visualization of Fermi's Golden Rule Through Imaging of Light Emission from Atomic Silver Chains

Chi Chen,[1] C. A. Bobisch,[2] W. Ho[1,2*]

VOL 325 21 AUGUST 2009

Atomic-scale spatial imaging of one-dimensional chains of silver atoms allows Fermi's golden rule, a fundamental principle governing optical transitions, to be visualized. We used a scanning tunneling microscope (STM) to assemble a silver atom chain on a nickel-aluminum alloy surface. Photon emission was induced with electrons from the tip of the STM. The emission was spatially resolved with subnanometer resolution by changing the tip position along the chain. The number and positions of the emission maxima in the photon images match those of the nodes in the differential conductance images of particle-in-a-box states. This surprising correlation between the emission maxima and nodes in the density of states is a manifestation of Fermi's golden rule in real space for radiative transitions and provides an understanding of the mechanism of STM-induced light emission.